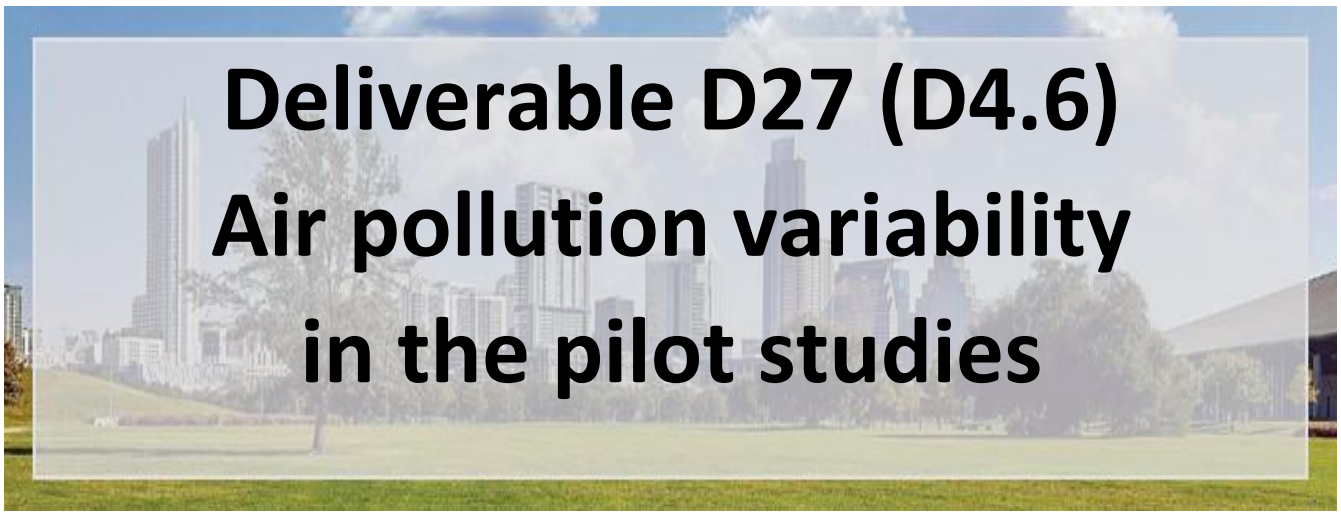

Deliverable D27 (D4.6)
Air pollution variability in the pilot studies

RI-URBANS

Research Infrastructures Services Reinforcing Air Quality Monitoring Capacities in European Urban & Industrial AreaS (GA n. 101036245)

By

CNRS, ENPC, UU, INOE, UoB, VITO & NOA

25 March 2024

RI-URBANS (www.RIURBANS.eu) is supported by the European Commission under the Horizon 2020 – Research and Innovation Framework Programme, H2020-GD-2020, Grant Agreement number: 101036245

Deliverable D27 (D4.6): Air pollution variability in the pilot studies

Authors: Karine Sartelet (CNRS/ENPC), Gerard Hoek (UU), Eleni Athanasopoulou (NOA), Roy M. Harrison (UoB), Alexandru Ilie (INOE), Jules Kerckhoffs (UU), Youngseob Kim (CNRS/ENPC), Lya Lugon (CNRS/ENPC), Doina Nicolae (INOE), Soo-Jin Park (CNRS/ENPC), Camelia Talianu (INOE), Martine Van Poppel (VITO), Jeni Vasilescu (INOE) & Jian Zhong (UoB)

Work package (WP)	WP4 Pilot implementations for testing and demonstrating services
Deliverable	D27 (D4.6)
Lead beneficiary	CNRS
Deliverable type	■ R (document, report) ☐ DEC (websites, patent filings, videos,….) ☐ Other: ORDP (open research data pilot)
Dissemination level	■ PU (public) ☐ CO (confidential, only members of consortium and European Commission))
Estimated delivery deadline	M30 (31/03/2024)
Actual delivery deadline	25/03/2024
Version	Final
Reviewed by	WP4 leaders and coordinators
Accepted by	Project coordination team
Comments	This document summarises the results of T4.3 from the WP4 of RI-URBANS on urban fine scale mapping including innovative modelling, monitoring, and crowdsourcing. This has taken advantage of developed Service Tools (STs) from WP1 to 3 for the European urban areas to describe the variability of outdoor exposure of ultrafine particles (UFP) and other pollutants using modelling tools, mobile measurements of UFP, black carbon (BC) and mid-cost sensors for measuring atmospheric particulate matter (PM), novel dispersion measurements, and the participation of networks of citizens and new innovative instruments by SMEs.

RI-URBANS (www.RIURBANS.eu) is supported by the European Commission under the Horizon 2020 – Research and Innovation Framework Programme, H2020-GD-2020, Grant Agreement number: 101036245

Table of Contents

RI-URBANS (www.RIURBANS.eu) is supported by the European Commission under the Horizon 2020 – Research and Innovation Framework Programme, H2020-GD-2020, Grant Agreement number: 101036245

1. About this document

T4.3 from the WP4 of RI-URBANS deals with urban fine scale mapping including innovative modelling, monitoring, and crowdsourcing. This has taken advantage of developed Service Tools (STs) from WP1 to 3 for the European urban areas to describe the variability of outdoor exposure of ultrafine particles (UFP) and other pollutants using modelling tools, mobile measurements of UFP, black carbon (BC) and mid-cost sensors for measuring atmospheric particulate matter (PM), novel dispersion measurements, and the participation of networks of citizens and new innovative instruments by SMEs. This document (D27(D4.6)) summarises the results of these mapping tasks.

This is a public document that will be distributed to all RI-URBANS partners for their use and submitted to European Commission as a RI-URBANS deliverable D27 (D4.6). This document can be downloaded at https://riurbans.eu/work-package-4/#deliverables-wp4

Different techniques may be used to provide high-resolution outdoor exposure city maps for pollutants related to health effects, using modelling tools, mobile measurements of nanoparticles, BC and PM mid-cost sensors, novel dispersion measurements, and the participation of networks of citizens and new innovative instruments. In cities, the urban background concentrations are often simulated with chemical transport models, which typically have horizontal resolutions coarser than 1 km x 1 km, and they cannot capture the city heterogeneities. Variability along traffic axes and streets is particularly important for NO_2, black carbon (BC), ultrafine particle (UFP) represented by the number of particles (PN), $PM_{2.5}$ and PM_{10}. This variability may differ depending on season, and a resolution below 100 m may be necessary to characterise them. Depending on the pilot city, two main approaches are used to represent these heterogeneities:

- Deterministic models with a multi-scale and multi-pollutant (NO_2, $PM_{2.5}$, PM_{10}, black carbon (BC), Number concentrations) approach (Paris, Birmingham and Athens).
- Analysis of mobile monitoring and/or citizen observations using Land Use Regression (LUR) modelling (Rotterdam, Bucharest) to map Number, $PM_{2.5}$, PM_{10}, NO_2 concentrations.

The modelled concentrations are evaluated against routine monitoring when possible. This is sometimes difficult because of the sparsity of monitoring data, especially for non-regulated pollutants. It is desirable to evaluate the models at different types of stations characteristic of urban areas (traffic, urban background, suburban). For cities using LUR modelling, only the mean concentrations may be compared to measurements. For cities using deterministic modelling, more detailed statistics of comparisons are performed, as daily concentrations are explicitly estimated: the root-mean-square-error (RMSE), the mean fractional bias (MFB), the mean fractional error (MFE), the correlation (R) and the factor 2 (FAC2) are estimated. FAC2 measures the fraction of estimates within a factor of two of the observations. Boylan and Russel (2006) defined a model performance criteria and goal, that is based in MFB and MFE: the model performance criteria are satisfied if MFE < 75% and MFB < ±50%, while the model performance goal is satisfied if MFE< 50% and MFB < ±30%. Note that the performance criteria and goal relate to both MFB and MFE, as errors may compensate to give a low bias. FAC2 should be as close to 1 as possible, and a model is estimated to perform relatively well if FAC2 is greater than 0.3 or 0.5 (Hanna and Chang, 2012).

RI-URBANS (www.RIURBANS.eu) is supported by the European Commission under the Horizon 2020 – Research and Innovation Framework Programme, H2020-GD-2020, Grant Agreement number: 101036245

To characterise the air pollution variability in the pilot cities, concentrations are mapped for a Winter and a Summer period, and the concentration differences between these two periods are compared.

The variability of concentrations for each pilot city is quantified using the normalised standard deviation (NSD). The NSD gives information about the variability of the local-scale concentrations. It is estimated within grid cells of 1 km x 1 km, as well as over specific areas, e.g. urban, suburban areas. As defined in the milestone M3.5, the normalised standard deviation (NSD) within a 1 km x 1 km grid can be written as

$$NSD = \frac{\sqrt{\frac{1}{n}\sum_{i,j}\left(C_{loc}(i,j) - \overline{C_{loc}}\right)^2}}{\overline{C_{loc}}}$$

where $\overline{C_{loc}}$ is the mean of the sub-grids and *n* the total number of sub-grids within the 1 km x 1 km grid or within the domain.

For cities using deterministic modelling with a chemistry-transport model to estimate urban background concentrations (Paris and Athens), the Normalised Mean Bias (NMB) may be used to quantify the differences between the sub-grid variability and the regional-scale urban background concentrations simulated with a chemistry-transport model (CTM) of 1 km x 1 km resolution:

$$NMB = \frac{\sum_{I,J\in D}\left(\overline{C_{loc}}(I,J) - C_{reg}(I,J)\right)}{\sum_{I,J\in D} C_{reg}(I,J)}$$

where *I,J* are the regional-grid indices.

To estimate the impact of the sub-grid variability on population exposure, and to provide a more realistic estimate of exposure within a grid, the sub-grid variability of (the health-related indicator of) population exposure to air pollution is calculated. Population exposure corresponds here to outdoor exposure. The outdoor population exposure is assessed by multiplying the population data at the residential address. The population weighted concentration (PWC) in any model grid *(I,J)* with sub-grids *(i,j)* within that grid, is calculated using the following equation

$$PWC(I,J) = \frac{\sum_{i\in I,j\in J}\ pop(i,j)\ C_{loc}(i,j)}{\sum_{i\in I,j\in J}\ pop(i,j)}$$

where *I,J* denote the 1 km x 1 km grid values, the *i,j* denote the sub-grid model values, and is the population with residential address within the grid cell i,j. The Exposure Scaling Factor (ESF) is defined as the ratio of the PWC to the regional scale concentration. This ESF may be used to correct regional-scale concentrations to provide a better estimate of the outdoor concentrations to which people are exposed.

First we present results from the individual pilot cities and then provide the summary of the results in the last section of this deliverable.

2. Paris Pilot

The concentration variability and outdoor population exposure in Paris are estimated using the multi-scale modelling chain CHIMERE/MUNICH/SSH-aerosol and the detailed population data from the MAJIC database (Letinois, 2014).

RI-URBANS (www.RIURBANS.eu) is supported by the European Commission under the Horizon 2020 – Research and Innovation Framework Programme, H2020-GD-2020, Grant Agreement number: 101036245

The urban background concentrations are simulated by the CHIMERE model (Menut et al. 2021) coupled to aerosol module SSH-aerosol (Sartelet et al. 2020), using nested domains down to Greater Paris. The domain of simulation is discretized with a 1 km x 1 km resolution and a zoom is performed down to the streets of Paris with the street-network model MUNICH (Lugon et al. 2021, Kim et al. 2022). As the same chemistry and aerosol module is used at the regional scale and in the street network, the representation of chemistry and aerosol dynamics is coherent at all scales, from the street to the background. As black carbon (BC) and Particulate Number (PN) are strongly influenced by traffic, a bottom-up approach is used for emissions, as detailed in the deliverable of WP3.1. The road traffic emissions data were produced by the Parisian air quality agency (Airparif) based on the results obtained using the Heaven system corrected from the count data received in near-real time. In the chain CHIMERE/MUNICH, the regional-scale traffic emissions were estimated by aggregating the local-scale emissions corrected from the local traffic counts.

For other activity sectors, the Aiparif inventory of 2019 was used. Number emissions were estimated from the Airparif inventory using the methodology detailed in Sartelet et al. (2022). Biogenic emissions were calculated using the Model of Emissions of Gases and Aerosols from Nature (MEGAN), as implemented in CHIMERE.

The MAJIC database is used to estimate the outdoor population exposure. This database determines the number of inhabitants in the different buildings of Paris city, crossing several databases, such as residential premises from the MAJIC property database and population statistics. The data is cross-referenced with IGN spatial databases (BD PARCELLAIRE and BD TOPO) and INSEE population statistics to estimate the number of inhabitants in each building. This methodology guarantees the consistency of the spatialization of the population.

2.1 Comparison of Summer and Winter concentrations

The multi-scale simulations are performed for Summer (from 1 June 2022 to 31 July 2022) and Winter (from 1 December 2020 to 31 January 2021). Figure 2.1 shows the NO_2, BC, $PM_{2.5}$, and PN (number of particles of diameters higher than 10 nm) concentrations for Summer and Winter using CHIMERE/MUNICH. The concentrations of NO_2 tend to be higher along streets with high traffic in both seasons (Figures 2.1a and 2.1b). The spatial distributions of BC, $PM_{2.5}$, and PN are similar to NO_2. The concentrations of NO_2, BC, $PM_{2.5}$, and PN are higher in Winter than in Summer, probably because the boundary layer height is lower in Winter, leading to an accumulation of anthropogenic pollutants emitted in the city. Also, during the Winter season, the contributions of residential emissions from heating tend to increase particle concentrations. In Winter, the difference in concentration between the background and street concentrations seems relatively lower compared to Summer, in particular for $PM_{2.5}$.

The simulated concentrations are evaluated by comparison to measurement stations using statistics such as Mean Fractional Bias (MFB), Mean Fractional Error (MFE), and root-mean-square error (RMSE) in Tables 2.1 to 2.4. For all pollutants and at all station types, the mean concentrations compare well to the observations satisfying the model performance criteria (MFE < 75%, MFB < ±50%) and in most cases the model performance goal (MFE< 50% and MFB < ±30%) of Boylan and Russell (2006). For comparisons to observations, as the model simulates EC, the EC concentrations are corrected to BC concentrations, using a harmonization factor, following Savadkoohi et al. (2023). A harmonization factor of 1.76 was determined for Paris in the Summer 2022 using EC and BC colocated measurements at Les Halles station, which is a urban background station operated by Airparif in the center of Paris. Although the modelled concentrations satisfy the model performance criteria for BC (Table 2.2), urban background BC is under-estimated during Wintertime at background stations, linked to uncertainties in the speciation of emissions from the residential sector. However, BC is very well modelled during Summertime and at traffic sites, satisfying the model performance goal. For NO_2 and $PM_{2.5}$, the CHIMERE/MUNICH reproduces the concentrations in both seasons well (Table 2.3), satisfying the model performance goal. PN concentrations are also well modelled. Note that there is no measurement of PN at traffic stations in Winter.

RI-URBANS (www.RIURBANS.eu) is supported by the European Commission under the Horizon 2020 – Research and Innovation Framework Programme, H2020-GD-2020, Grant Agreement number: 101036245

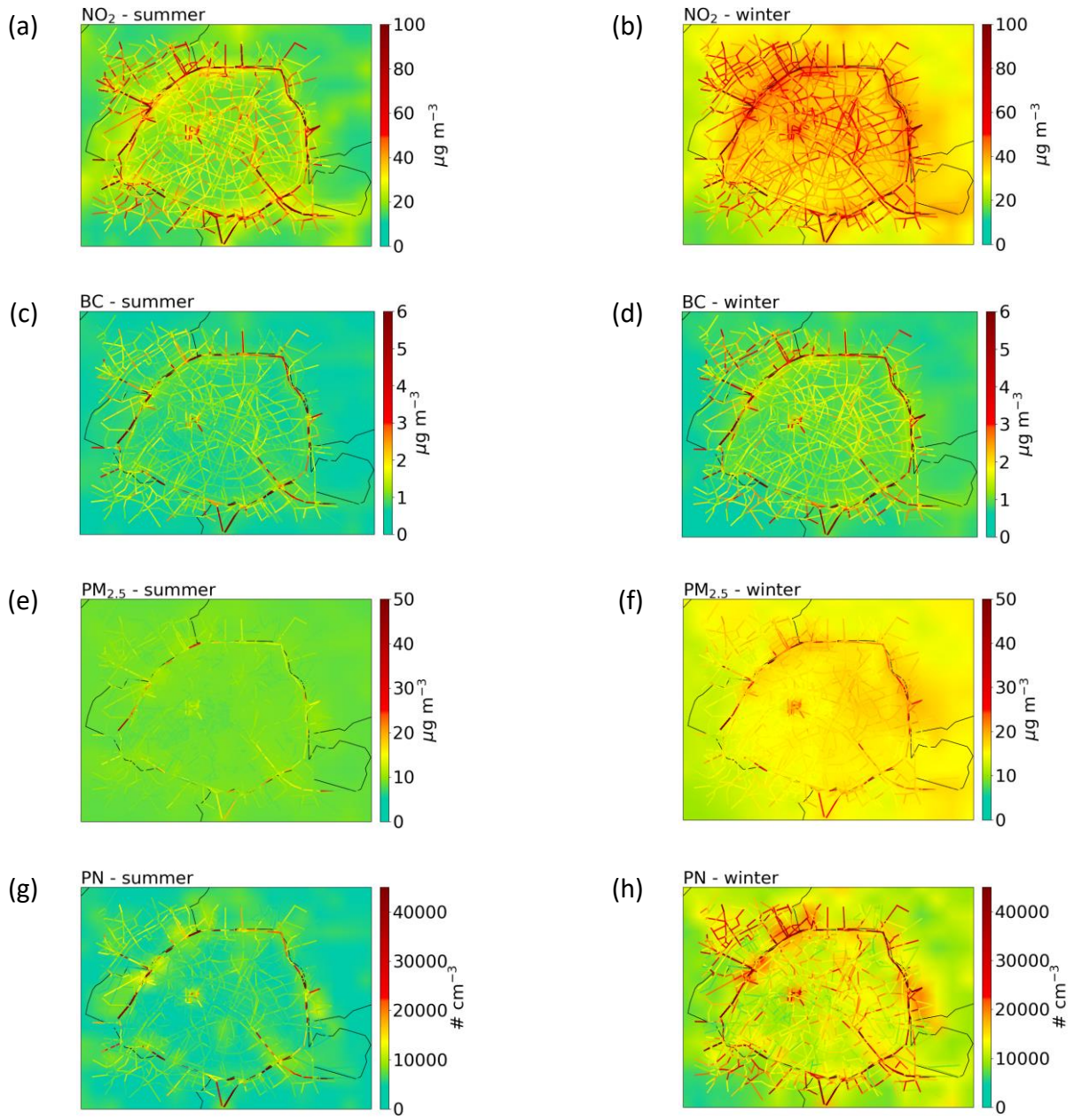

Figure 2.1. *NO_2 [(a) and (b)], BC [(c) and (d)], $PM_{2.5}$ [(e) and (f)], and PN [(g) and (g)] concentrations simulated for Summer (left panels) and Winter (right panels) using CHIMERE/MUNICH.*

RI-URBANS (www.RIURBANS.eu) is supported by the European Commission under the Horizon 2020 – Research and Innovation Framework Programme, H2020-GD-2020, Grant Agreement number: 101036245

Table 2.1. *NO_2 model to measurement comparisons at background and traffic stations for Summer and Winter.*

NO_2	station	Stat. Type	Obs. (μg m^{-3})	Sim. (μg m^{-3})	MFE (%)	MFB (%)	RMSE (μg m^{-3})	FAC2 (%)	R (%)
Summer	Urban	21	15.0	15.6	34	5	6.7	88	52
	Traffic	10	40.0	41.0	26	4	13.9	93	69
Winter	Urban	21	24.7	26.7	30	5	9.1	92	75
	Traffic	9	42.2	51.7	30	22	16.1	93	50

Table 2.2. *BC model to measurement comparisons at background and traffic stations for Summer and Winter.*

BC	station	Stat. Type	Obs. (μg m^{-3})	Sim. (μg m^{-3})	MFE (%)	MFB (%)	RMSE (μg m^{-3})	FAC2 (%)	R (%)
Summer	Urban	4	0.77	0.72	50	0	0.5	63	48
	Traffic	3	2.26	1.99	37	4	1.0	93	81
Winter	Urban	5	1.10	0.70	47	-38	0.7	67	53
	Traffic	2	3.09	2.89	45	10	1.7	75	49

Table 2.3. *$PM_{2.5}$ model to measurement comparisons at background and traffic stations for Summer and Winter.*

PM2.5	station	Stat. Type	Obs. (μg m^{-3})	Sim. (μg m^{-3})	MFE (%)	MFB (%)	RMSE (μg m^{-3})	FAC2 (%)	R (%)
Summer	Urban	8	7.2	8.3	33	21	3.1	88	61
	Traffic	3	11.2	11.8	20	7	2.9	97	65
Winter	Urban	8	11.2	12.1	41	17	6.2	81	69
	Traffic	2	16.3	18.5	29	18	6.2	94	67

Table 2.4. *PN model to measurement comparisons at background and traffic stations for Summer and Winter.*

PN	station	Stat. Type	Obs. (# m^{-3})	Sim. (# m^{-3})	MFE (%)	MFB (%)	RMSE (# m^{-3})	FAC2 (%)	R (%)
Summer	Urban	3	8145	5843	41	-34	3562	95	63
	Traffic	1	9141	7713	23	-13	2521	100	73
Winter	Urban	4	7396	7342	32	0	3057	96	60
	Traffic	-	-	-	-	-	-	-	-

RI-URBANS (www.RIURBANS.eu) is supported by the European Commission under the Horizon 2020 – Research and Innovation Framework Programme, H2020-GD-2020, Grant Agreement number: 101036245

2.2 Variability within 1 km x 1km areas

Although the spatial distributions of NO_2, BC, $PM_{2.5}$, and PN seem similar from the maps displayed in the previous section, their sub-grid variability is quantified using the normalised standard deviation (NSD) and the normalised mean bias (NMB). The NSD gives information about the variability of the concentrations at the local scale, while the NMB compares the differences between regional and average local-scale concentrations.

The distributions of NSD for BC and PN are similar between Summer and Winter (Figure 2.2), despite higher concentrations observed in Winter compared to Summer (Figure 2.1). The NSD is relatively higher in grids that include high-traffic roads (Paris ring roads). This indicates the relatively high concentration differences between Paris ring roads and surrounding streets. For BC, $PM_{2.5}$, and PN, the NSD is similar between Summer and Winter, except for NO_2 (Table 2.5). NO_2 concentrations in Winter are high on most roads in Paris (Figure 2.1), with relatively small differences in concentrations between roads, resulting in low NSD in Winter compared to Summer. $PM_{2.5}$ has a lower variability of concentration between roads compared to NO_2, BC, and PN in both seasons.

The distribution and average NMB have similar tendencies as NSD (Figure 2.2 and Table 2.5). The NMB also tends to be higher along the Paris ring road compared to the city centre. The NMB is very high for BC and NO_2 in Winter, indicating bias as large as 75-87% between the regional-scale concentrations and the local-scale ones for BC. The NMB is high for PN as well, ranging between 38% and 45% in average. The NMB for $PM_{2.5}$ is lower than for other pollutants, about 9%. As for the NSD, the NMB is similar in Winter and Summer, except for NO_2 for which the NMB is lower in Winter compared to Summer.

Table 2.5. *Average NSD and NMB of NO_2, BC, $PM_{2.5}$, and PN in Paris for Summer and Winter.*

Paris	NSD				NMB			
	NO_2	BC	$PM_{2.5}$	PN	NO_2	BC	$PM_{2.5}$	PN
Summer	0.27	0.27	0.07	0.25	0.75	0.75	0.09	0.45
Winter	0.14	0.27	0.06	0.29	0.36	0.83	0.09	0.38

RI-URBANS (www.RIURBANS.eu) is supported by the European Commission under the Horizon 2020 – Research and Innovation Framework Programme, H2020-GD-2020, Grant Agreement number: 101036245

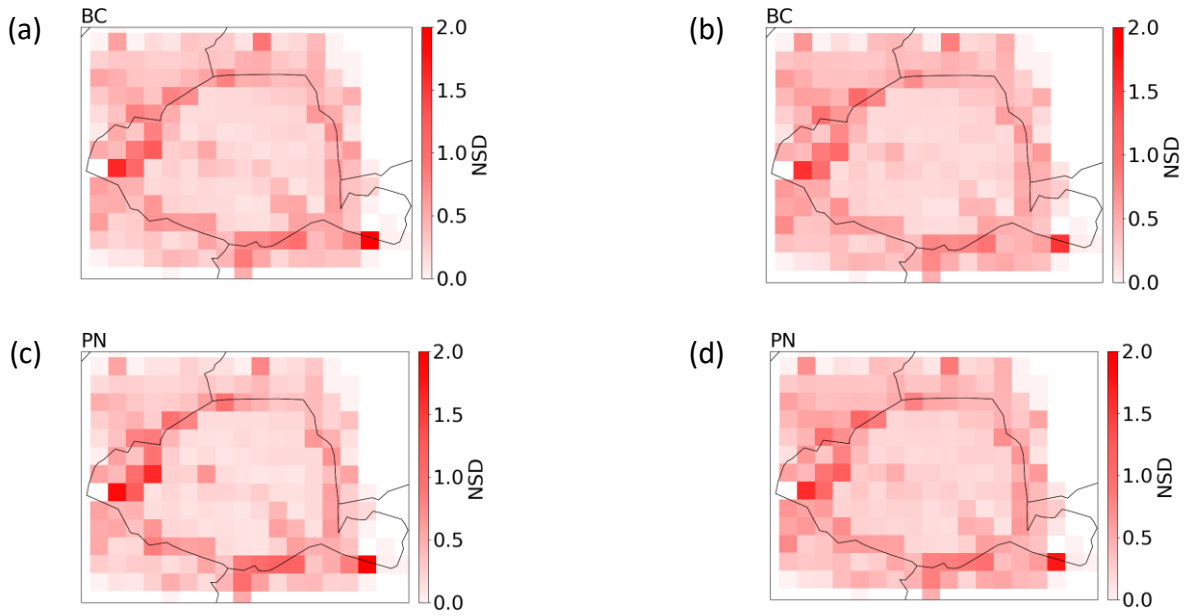

Figure 2.2. *NSD of BC [(a) and (b)] and PN [(c) and (d)] in Summer (left panels) and Winter (right panels).*

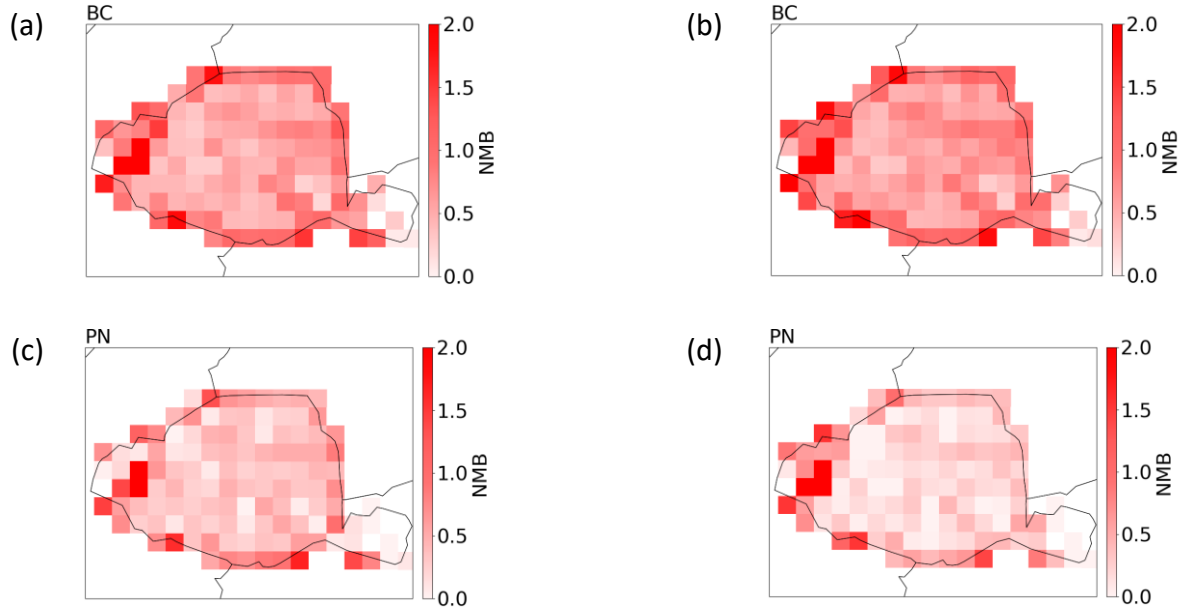

Figure 2.3. *NMB of BC [(a) and (b)] and PN [(c) and (d)] in Summer (left panels) and Winter (right panels).*

The NSD and NMB are averaged over specific areas, focusing on Paris ring roads, which are roads with heavy traffic, and the city centre. As seen in Figure 2.2, the NSD along Paris ring roads are more than twice higher than in the city centre (Table 2.6). The NSD along Paris ring roads is highest for PN, BC, NO_2, and $PM_{2.5}$ in order, while in the city centre, it is highest for BC, NO_2, PN, and $PM_{2.5}$ in order. The NMB is higher along Paris ring roads than in the city centre (Table 2.7). For BC, $PM_{2.5}$, and PN, the NMB along the Paris ring roads is more than twice that in the city centre. The NMB for BC along Paris ring roads is very high in Summer and Winter, at 1.07 and 1.15, respectively. NO_2 has a relatively small difference between Paris ring roads and the city centre compared to other pollutants.

RI-URBANS (www.RIURBANS.eu) is supported by the European Commission under the Horizon 2020 – Research and Innovation Framework Programme, H2020-GD-2020, Grant Agreement number: 101036245

Table 2.6. *Average NSD of NO_2, BC, $PM_{2.5}$, and PN in Paris ring roads and city centre for Summer and Winter.*

NSD	Paris ring roads				City center			
	NO_2	BC	$PM_{2.5}$	PN	NO_2	BC	$PM_{2.5}$	PN
Summer	0.51	0.65	0.21	0.69	0.24	0.22	0.05	0.18
Winter	0.36	0.62	0.18	0.67	0.11	0.22	0.05	0.24

Table 2.7. *Average NMB of NO_2, BC, $PM_{2.5}$, and PN in Paris ring roads and city centre for Summer and Winter.*

NMB	Paris ring roads				City centre			
	NO_2	BC	$PM_{2.5}$	PN	NO_2	BC	$PM_{2.5}$	PN
Summer	0.84	1.07	0.16	0.70	0.67	0.50	0.04	0.27
Winter	0.46	1.15	0.15	0.55	0.25	0.58	0.05	0.14

2.3 Variability of population exposure and exposure scaling factor

The population-weighted concentration (PWC) and exposure scaling factor (ESF) are calculated for Paris city. The PWC is calculated by weighting populations by the concentration to which they are exposed at the precise location of their home. People living in a building that is on the main street are assigned to that street concentration. People living in a building that does not open directly onto the street are assigned to urban background concentrations. The ESF is defined as the ratio of the PWC to the regional scale concentration.

As concentrations of NO_2, BC, $PM_{2.5,}$ and PN are higher in Winter than in Summer, the PWC is also higher in Winter than in Summer for these pollutants, and it is particularly high along Paris ring roads (Figure 2.4). The spatial distributions of PWC for all pollutants are similar to their concentrations. The average PWC in Paris during Winter is between 1.2 to 2.0 times higher than in Summer (Table 2.8), reaching the factor 2.0 for the PWC of PN. The PWC of BC in Winter is 1.2 times higher than in Summer, this is the smallest difference among the pollutants.

Although the PWC in Winter is higher than in Summer, the ESF is similar in both seasons (Figure 2.5). The ESF is highest for NO_2, BC, PN, and $PM_{2.5}$ in order, and the average ESF in Paris is higher than 1 for all pollutants in both Summer and Winter (Table 2.8). A ESF value higher than 1 indicates that the concentrations simulated at the local scale in streets are higher than those modelled at the regional scale. For $PM_{2.5}$, the ESF (1.03) is close to 1, corresponding to the lowest difference between regional and local scale concentrations, as shown in Figure 1. The ESF is the highest for BC (between 1.29 and 1.34), indicating that outdoor population exposure is under-estimated by as much as 30% when considering regional-scale concentrations.

RI-URBANS (www.RIURBANS.eu) is supported by the European Commission under the Horizon 2020 – Research and Innovation Framework Programme, H2020-GD-2020, Grant Agreement number: 101036245

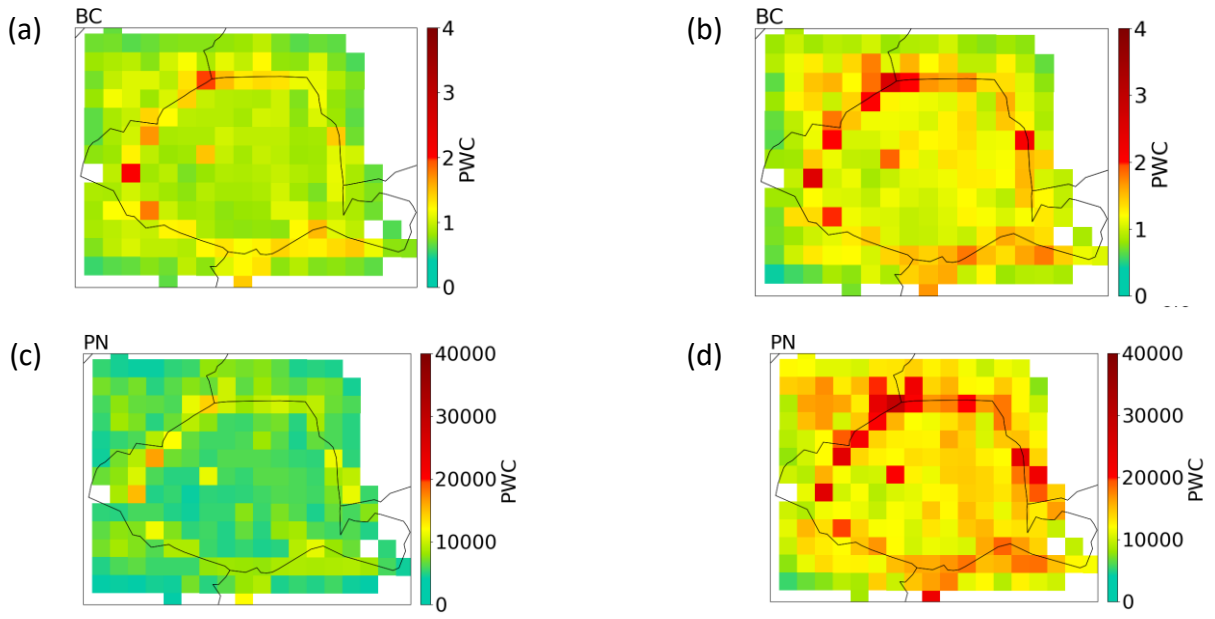

Figure 2.4. *PWC of BC [(a) and (b)] and PN [(c) and (d)] in Summer (left panels) and Winter (right panels).*

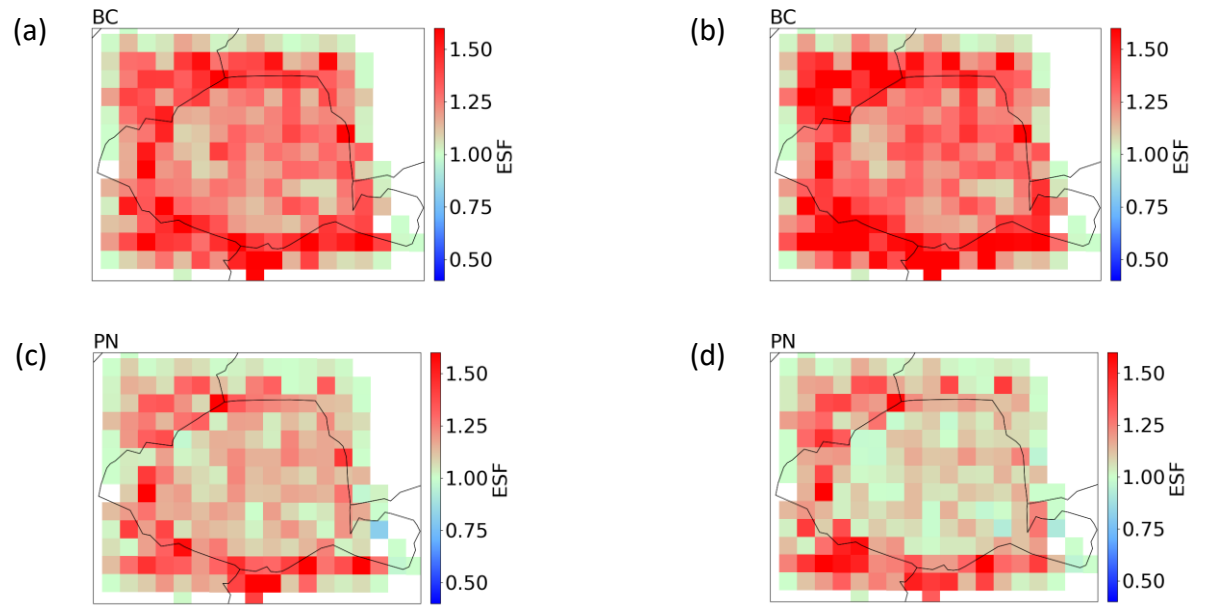

Figure 2.5. *ESF of BC [(a) and (b)] and PN [(c) and (d)] in Summer (left panels) and Winter (right panels).*

Table 2.8. *Average PWC and ESF of NO_2, BC, $PM_{2.5}$, and PN in Paris for Summer and Winter.*

Paris	PWC				ESF			
	NO_2	BC	$PM_{2.5}$	PN	NO_2	BC	$PM_{2.5}$	PN
Summer	26.4	1.02	9.3	7047	1.31	1.29	1.03	1.18
Winter	40.5	1.27	16.2	14110	1.14	1.34	1.04	1.13

RI-URBANS (www.RIURBANS.eu) is supported by the European Commission under the Horizon 2020 – Research and Innovation Framework Programme, H2020-GD-2020, Grant Agreement number: 101036245

2.4 Comparisons of the variability of pollutants

Figure 2.6 shows the ratio of pollutant concentrations. They are based on a quantile division of each of the two pollutants and their relative loading. So each of the four colours represents an equal number of street segments. High NO_2, BC and PN are observed along the main roads. Low NO_2, BC and PN are observed in areas far from the roads.

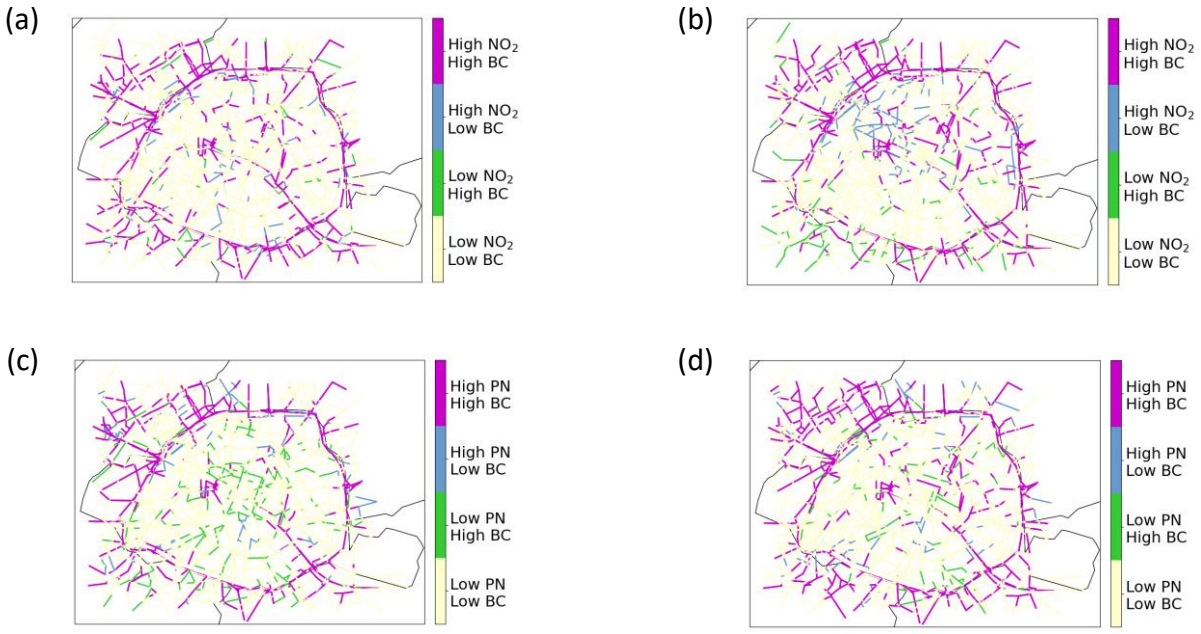

Figure 2.6. *Ratios of NO_2/BC [(a) and (b)] and PN/BC [(c) and (d)] in Summer (left panels) and Winter (right panels).*

3. Birmingham Pilot

The local scale ADMS-Urban dispersion model has been used for the Birmingham Pilot to generate high resolution air quality datasets for NO_2, $PM_{2.5}$ and UFPs (Zhong et al., 2021; Zhong et al., 2023). The ADMS-Urban is a quasi-Gaussian plume air dispersion model that represents the structure of the atmospheric boundary layer using meteorological parameters. Birmingham Airport site is an appropriate synoptic meteorological measurement site, which was used to drive the atmospheric dispersion in the model. Background concentration files were created using observation data from a variety of rural background sites (available via the UK Automatic Urban and Rural Network, AURN) surrounding the West Midlands modelling area. The upwind background site for each hour over the year was selected based on the monitored wind direction at that hour for NO_2, and $PM_{2.5}$. For UFPs, the number of AURN sites in the UK is very limited, and an appropriate background site with available UFPs data is Chilbolton (to inform the modelling background). For NO_2, and $PM_{2.5}$, the emission inventories were derived based on the UK NAEI emissions at a spatial resolution of 1 km × 1 km. Unlike emission inventories for traditional air pollutants (e.g. NO_2 and $PM_{2.5}$), there are limited sources for the emission inventory for UFPs in the UK. Such an emission inventory for UFPs has been developed by TNO in the RI-Urbans project and the 6 km × 6 km resolution emissions have been used in the Birmingham Pilot modelling study. For the explicit major road emissions, the local traffic model datasets have been obtained from Transport for West Midlands and Birmingham City Council. An Atmospheric Emissions Inventory Toolkit (EMIT developed by Cambridge Environmental Research Consultants, CERC) has been used to pre-process all types of emission sources before these can be used by the ADMS-Urban model. The advanced street

RI-URBANS (www.RIURBANS.eu) is supported by the European Commission under the Horizon 2020 – Research and Innovation Framework Programme, H2020-GD-2020, Grant Agreement number: 101036245

canyon and urban canopy module was applied to account for the local street canyon effect for road emissions and spatially varying urban canopy flow for all source types. A novel task farming approach was implemented to enable the parallel running of the same or sequential code with different modelling parameters and inputs on multiple cores on supercomputer clusters at the University of Birmingham. The baseline modelling for the year of 2019 has been evaluated against local air quality measurement sites using a Model Evaluation Toolkit (developed by CERC) with good model performance. The model can generate high resolution air quality maps at 10 m x 10 m, which can be used to investigate spatial and temporal concentration variability.

3.1 Comparison of Summer and Winter concentrations

The ADMS-Urban model was performed for the whole year of 2019. Summer and Winter concentrations can be extracted and compared. Here, Summer represents the months of June, July and August 2019, while Winter is for the months of January, February and December 2019. Figure 3.1 shows the comparison of Summer and Winter concentrations for NO_2, $PM_{2.5}$, and PN. There were relatively higher concentrations of NO_2, $PM_{2.5}$, and PN near motorways and major roads in city centre areas, mostly due to the higher traffic-related emissions. This finding was also indicated in the Paris pilot. Away from major roads and in rural areas, concentrations were generally lower. The modelled concentrations of NO_2, $PM_{2.5}$, and PN are relatively higher in Winter than these in Summer, which was also found in other pilots. In Winter, the boundary layer height is relatively lower and the atmosphere may have more stable occurrence due to the lower temperature. Also, there might be more activity of residential emissions (e.g. wood burning) in Winter, which will largely contribute to PM concentrations. In Summer, the atmosphere tends to be more unstable due to more surface heating from the sun, which will enhance the local dispersion.

The model performance was evaluated against local measured concentrations obtained from UK AURN and Birmingham Air Quality Supersite (BAQS) using the Model Evaluation Toolkit. These station types are classified as roadside and urban background stations. The Model Evaluation Toolkit calculates statistics from the hourly modelled and measured concentrations. The model evaluation statistics are shown in Tables 3.1, 3.2, and 3.3. For NO_2, $PM_{2.5}$, the measured concentrations were well captured by the model and there are small MFB, i.e. between -11% and 13%. For PN, MFB is larger between -44% and 32%. It is noted that there is only one measurement station (from BAQS) with available PN data for model evaluation. For Paris pilot, MFB for PN ranges between -13% and -34%. For all pollutants and all station types, RMSE in Summer is higher than that in Winter, but the correlation in Summer is lower than that in Winter. Fac2 (the fraction of modelled data within a factor of 2 of observations) is larger than 76% for NO_2 and $PM_{2.5}$, and larger than 61% for PN.

(a)

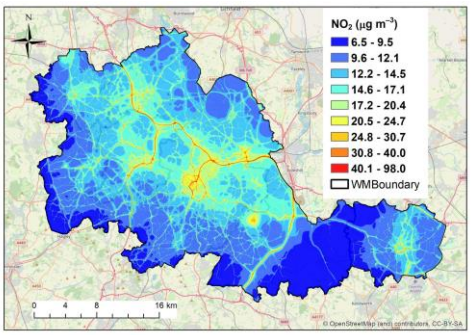

(b)

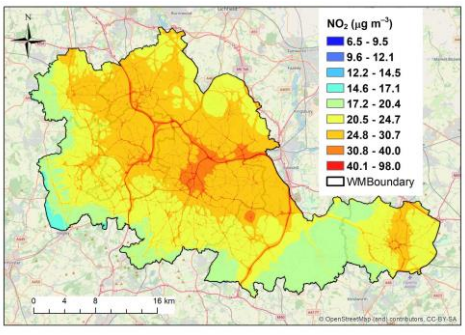

RI-URBANS (www.RIURBANS.eu) is supported by the European Commission under the Horizon 2020 – Research and Innovation Framework Programme, H2020-GD-2020, Grant Agreement number: 101036245

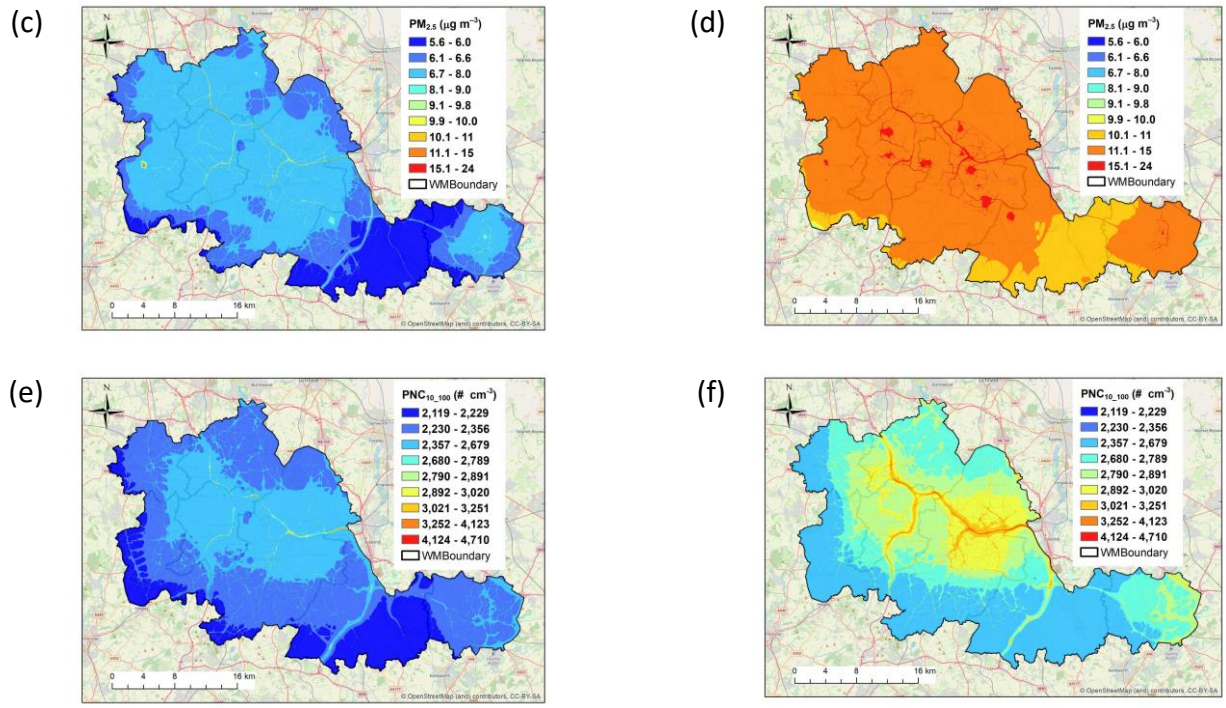

Figure 3.1. *NO_2 [(a) and (b)], $PM_{2.5}$ [(c) and (d)], and PN [(e) and (f)] concentrations simulated for Summer (left panels) and Winter (right panels) using ADMS-Urban.*

Table 3.1. *NO_2 model to measurement comparisons at background and roadside stations for Summer and Winter.*

NO_2	Station type	No of stations	Obs. (µg m^{-3})	Sim. (µg m^{-3})	MFB (%)	RMSE (µg m^{-3})	R	Fac2
Summer	Roadside	3	25.6	23.6	-8	13.7	0.54	0.82
	Background	5	12.4	13.7	10	9.6	0.51	0.77
Winter	Roadside	3	40.4	35.8	-11	19.3	0.68	0.81
	Background	5	25.0	24.8	-1	14.9	0.67	0.80

Table 3.2. *$PM_{2.5}$ model to measurement comparisons at background and roadside stations for Summer and Winter.*

$PM_{2.5}$	Station type	No of stations	Obs. (µg m^{-3})	Sim. (µg m^{-3})	MFB (%)	RMSE (µg m^{-3})	R	Fac2
Summer	Roadside	1	6.8	7.5	9	4.3	0.58	0.86
	Background	4	6.6	6.7	1	5.3	0.49	0.84

RI-URBANS (www.RIURBANS.eu) is supported by the European Commission under the Horizon 2020 – Research and Innovation Framework Programme, H2020-GD-2020, Grant Agreement number: 101036245

Winter	Roadside	1	12.7	14.3	13	9.6	0.60	0.77
	Background	4	11.7	12.8	10	8.2	0.59	0.76

Table 3.3. *PN model to measurement comparisons at background and roadside stations for Summer and Winter.*

PN	Station type	No of stations	Obs. (# cm^{-3})	Sim. (# cm^{-3})	MFB (%)	RMSE (# cm^{-3})	R	Fac2
Summer	Background	1	3396	2167	-44	2512	0.30	0.61
Winter	Background	1	1719	2364	32	1590	0.70	0.69

3.2 Variability within 1 km x 1km areas

The 10 m x 10 m air quality maps can be further aggregated into 1 km x 1 km resolution grids to investigate the sub-grid variability. It is noted that the analysed variability here at 1 km x 1 km resolution is purely based on these modelled 10 m x 10 m data. The NSD is the standard deviation of all 10 m x 10 m cells within each 1 km x 1 km grid normalised by the average of each 1 km x 1 km grid. The NSD reflects the variability of the concentrations at the local scale, which are not well captured by regional models. Figure 3.2 shows that the patterns of NSD for NO_2, $PM_{2.5}$, and PN are similar, with higher values for grids containing motorways or major roads with higher traffic. NO_2 has higher NSD than $PM_{2.5}$ followed by PN for both Summer and Winter. For NO_2 and $PM_{2.5}$, NSD in Summer is relatively higher than that in Winter. For PN, the NSD is similar between Summer and Winter. Table 3.4 further shows the domain averaged NSD (over Figure 3.2) of all pollutants for Summer and Winter. For all pollutants, the domain averaged NSD in Summer is generally higher than that in Winter for all pollutants.

Table 3.4. *Domain averaged NSD of all pollutants for Summer and Winter.*

Domain averages	*NSD*		
	NO_2	*$PM_{2.5}$*	*PN*
Summer	*0.14*	*0.03*	*0.015*
Winter	*0.07*	*0.02*	*0.014*

RI-URBANS (www.RIURBANS.eu) is supported by the European Commission under the Horizon 2020 – Research and Innovation Framework Programme, H2020-GD-2020, Grant Agreement number: 101036245

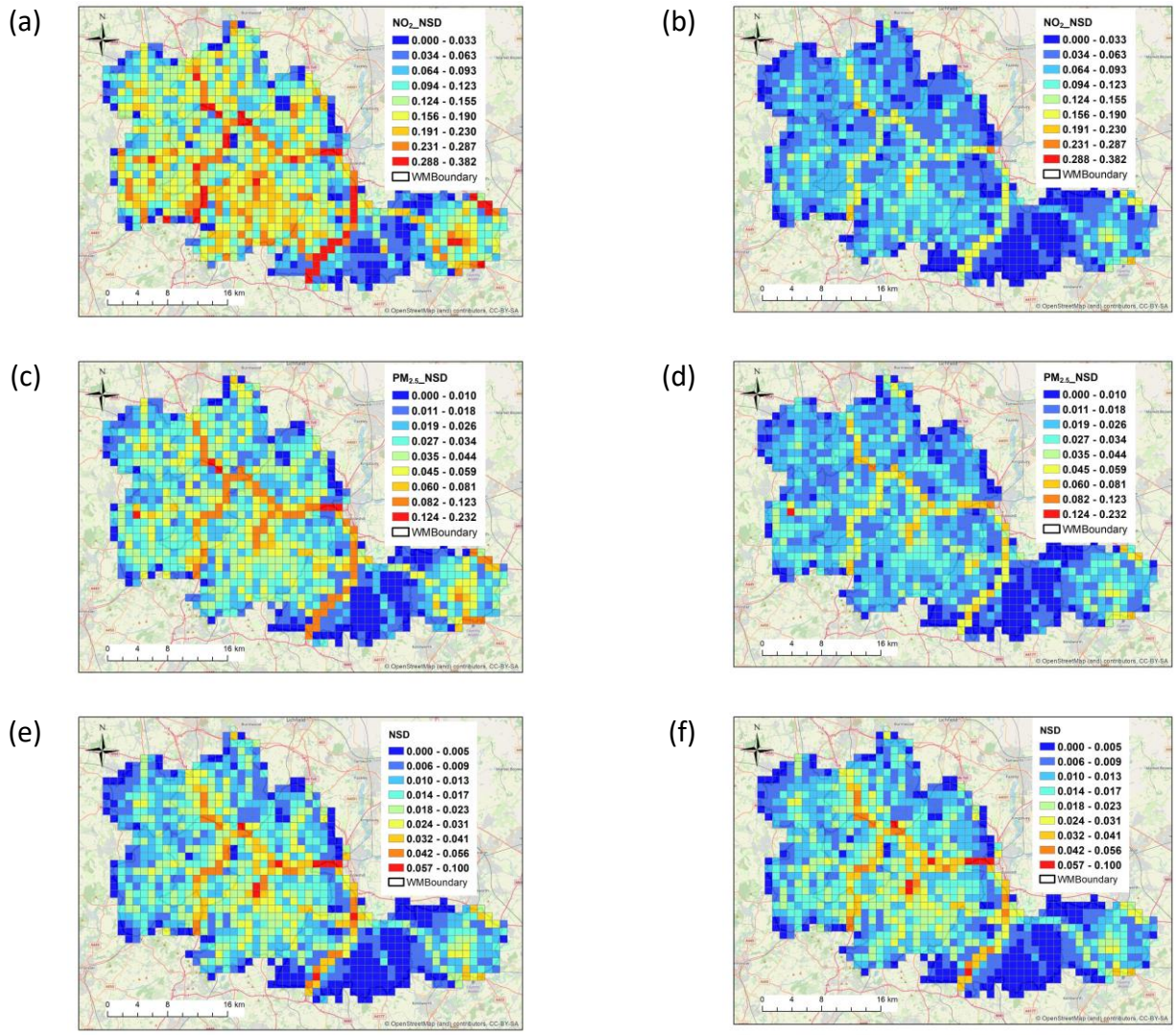

Figure 3.2. *NSD of NO_2 [(a) and (b)], $PM_{2.5}$ [(c) and (d)], and PN [(e) and (f)] for Summer (left panels) and Winter (right panels) using ADMS-Urban.*

3.3 Variability within specific areas

The 10 m x 10 m air quality maps can be also aggregated into regional local authorities level in order to investigate the variability within specific areas in the region. Table 3.5 shows NSD of NO_2, $PM_{2.5}$, and PN within specific local authorities for Summer and Winter. NSD of NO_2 is generally higher than that of $PM_{2.5}$ for both Summer and Winter, while NSD of PN is the lowest. For NO_2, NSD in Summer is higher than that in Winter for all local authorities. For $PM_{2.5}$, NSD in Summer is generally lower than that in Winter for 5 of the 7 local authorities in the region. For PN, NSD in Summer is lower than that in Winter for all local authorities.

RI-URBANS (www.RIURBANS.eu) is supported by the European Commission under the Horizon 2020 – Research and Innovation Framework Programme, H2020-GD-2020, Grant Agreement number: 101036245

Table 3.5. *NSD of all pollutants within specific local authorities (LA) for Summer and Winter.*

LA NAME	NO_2		$PM_{2.5}$		PN	
	Summer	Winter	Summer	Winter	Summer	Winter
Coventry	0.268	0.144	0.085	0.091	0.026	0.032
Dudley	0.271	0.158	0.085	0.089	0.035	0.048
Sandwell	0.239	0.135	0.063	0.053	0.033	0.035
Solihull	0.355	0.196	0.083	0.092	0.040	0.049
Walsall	0.230	0.121	0.070	0.062	0.031	0.032
Wolverhampton	0.226	0.143	0.058	0.069	0.028	0.040
Birmingham	0.291	0.173	0.080	0.088	0.045	0.060

3.4 Variability between pollutants

The variability between pollutants was reflected by the ratios between pollutants for both Summer and Winter, shown in Figure 3.3. The colour scales indicate a quantile division of these ratios, which means that each of these 4 colours represents an equal number of 10m x 10 m grids. Higher ratios between predicted NO_2 and $PM_{2.5}$ or PN are more restricted to the city centre and areas near motorways, which are more influenced by higher traffic induced NO_2. Higher ratios between predicted $PM_{2.5}$ and PN occur more in city centre areas with higher residential emissions and are less influenced by local traffic. These patterns of ratios between all pollutants are similar for Summer and Winter, with slight shifts possibly influenced by the local meteorology to some extent.

RI-URBANS (www.RIURBANS.eu) is supported by the European Commission under the Horizon 2020 – Research and Innovation Framework Programme, H2020-GD-2020, Grant Agreement number: 101036245

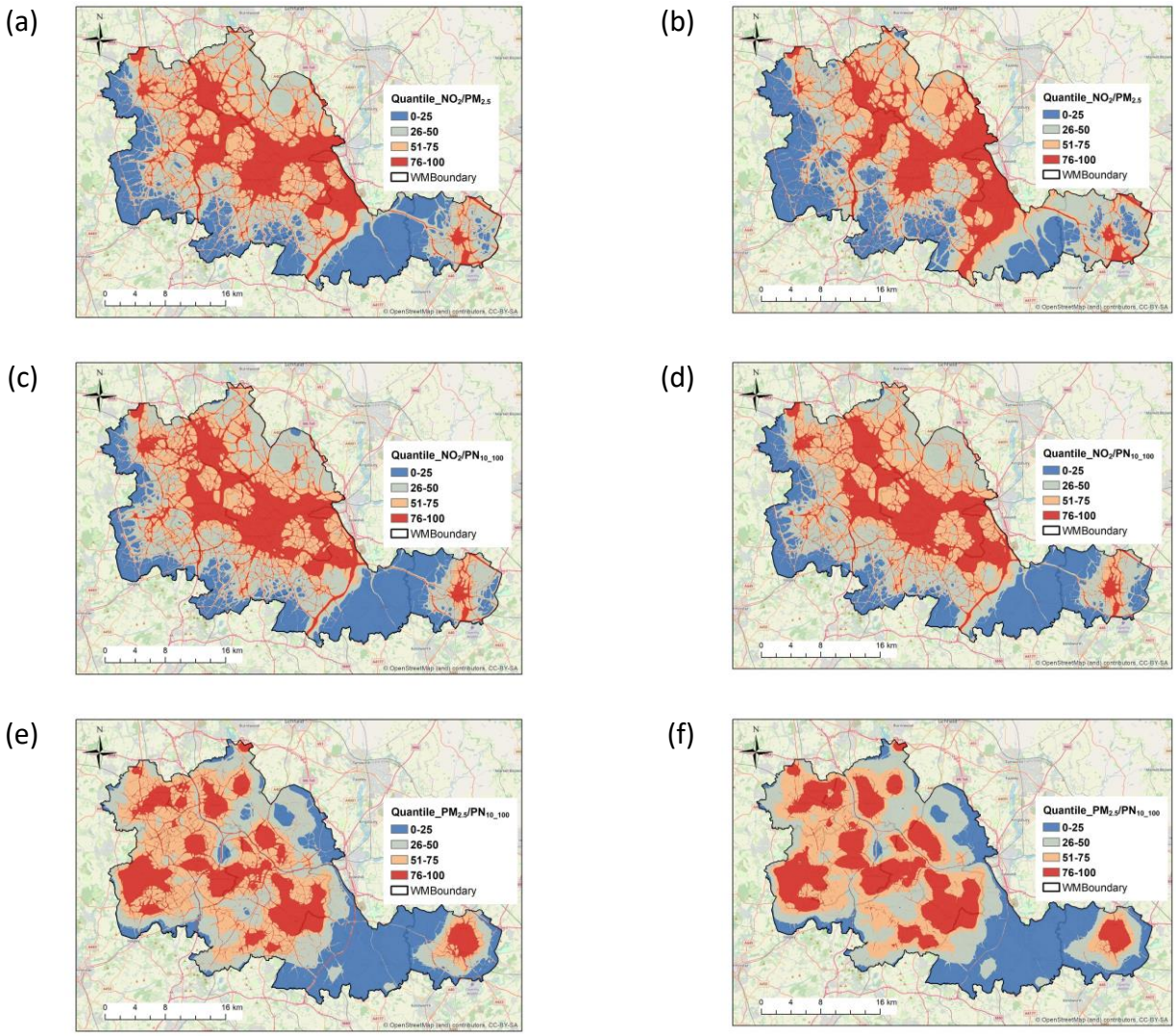

Figure 3.3. *Ratio between predicted NO_2 and $PM_{2.5}$ concentrations[(a) and (b)], Ratio between predicted NO_2 and PN concentrations [(c) and (d)], and Ratio between predicted $PM_{2.5}$ and PN concentrations [(e) and (f)] for Summer (left panels) and Winter (right panels) using ADMS-Urban.*

RI-URBANS (www.RIURBANS.eu) is supported by the European Commission under the Horizon 2020 – Research and Innovation Framework Programme, H2020-GD-2020, Grant Agreement number: 101036245

4. Athens Pilot

The concentration variability and outdoor population exposure to air pollution in Athens was assessed using the multi-scale numerical atmospheric model system CAMS/WRF/EPISODE-CityChem and the population data from the Global Human Settlement Layer (GHSL, https://ghsl.jrc.ec.europa.eu/). The core of the system is the chemistry transport model EPISODE-CityChem (Karl et al., 2019). Its comprehensive chemistry scheme is designed for treating complex atmospheric chemistry in urban areas and improved representation of the near-field dispersion. Input data (meteorology, boundary conditions, emissions) are heavily supported by Copernicus-related products. The model performs a specialized treatment on road and over the adjacent urban áreas. Specifically, it is fed with hourly road network emissions in a linear format, applies a Gaussian dispersion scheme in the street canyons, and an extra photochemical scheme over the greater area of road surfaces, gridded in 100 m-by-100 m cells. These two schemes are superimposed to the Eulerian treatment of atmospheric processes in the whole 3D urban domain, with a horizontal spatial resolution of 1 km and a 24-layered atmosphere up to 3.7 km.

Local-scale atmospheric simulations are performed for 2019, which is a recent year, free of Covid-related activity restrictions, and with a wind field representative of 2016-2020. Numerical predictions have been evaluated against local air quality measurements from the National regulatory network and from the Panacea RI, using evaluation statistics, comparative time-series plots and selected outputs from the application of the benchmarking methodology developed in the framework of the Forum for Air Quality Modelling in Europe (FAIRMODE). Air quality maps at 1km and at 100m resolution are used to investigate spatial and temporal concentration variability.

4.1 Comparison of summer and winter concentrations

The month used to represent summer is July and for winter is January. Figure 4.1 shows the NO_2 and $PM_{2.5}$ high resolution (100m) concentrations for a mean day in summer and winter as predicted by EPISODE-CityChem. The concentrations of NO_2 tend to be higher along streets with high traffic in both seasons (Figures 4.1a and 4.1b). The spatial distribution of both pollutants is similar with higher NO_2 than $PM_{2.5}$ values at the inner-city center. The concentrations are higher in winter than in summer, especially for $PM_{2.5}$ (and for background NO_2). The contributions of residential emissions from heating tend to increase particle concentrations during wintertime. NO_2 photochemistry is enhanced in Athens during summer-time, which is partly the reason for higher NO_2 concentrations at the traffic sites. Other reasons for seasonal differences include the lower boundary layer during wintertime and the stronger dispersion phenomena during summertime (incl. Etesian winds), which affect concentrations, mainly downwind the road network.

The simulated concentrations (in 100m cells) are evaluated by comparison to measurement stations using statistics such as Mean Fractional Bias (MFB), Mean Fractional Error (MFE), and root-mean-square error (RMSE) in Tables 4.1 and 4.2. For the 2 pollutants and station types, the mean concentrations compare well to the observations satisfying the model performance criteria (MFE < 75%, MFB < ±50%) and the model performance goal (MFE< 50% and MFB < ±30%) of Boylan and Russell (2006) in most cases.

RI-URBANS (www.RIURBANS.eu) is supported by the European Commission under the Horizon 2020 – Research and Innovation Framework Programme, H2020-GD-2020, Grant Agreement number: 101036245

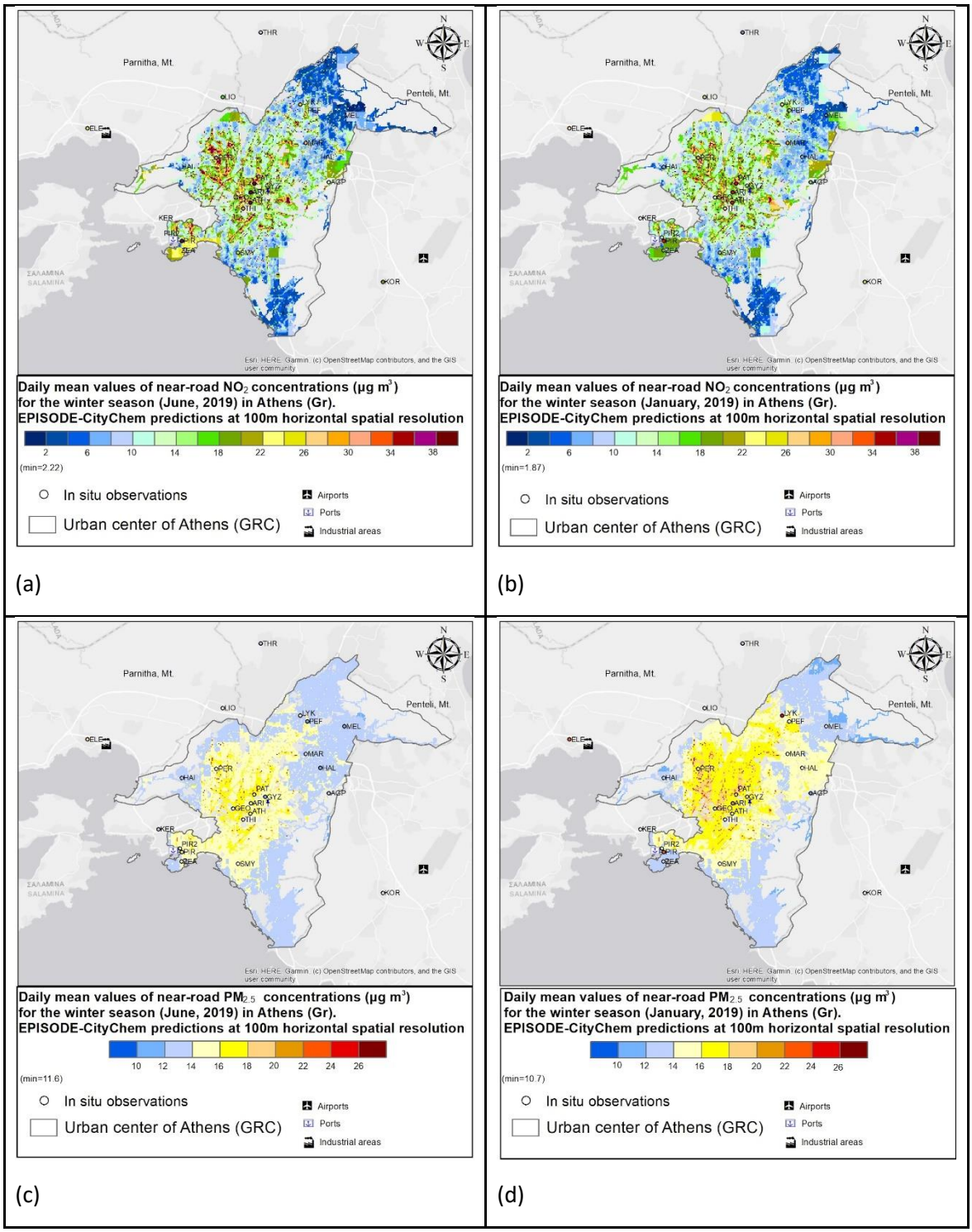

Figure 4.1. *NO_2 [(a) and (b)], $PM_{2.5}$ [(c) and (d)], near-road concentrations (µg m-3) over Athens simulated for summer (left panels) and winter (right panels) using EPISODE-CityChem.*

RI-URBANS (www.RIURBANS.eu) is supported by the European Commission under the Horizon 2020 – Research and Innovation Framework Programme, H2020-GD-2020, Grant Agreement number: 101036245

Table 4.1. *NO_2 model to measurement comparisons at (urban) background and (traffic) roadside stations in Athens for summer and winter.*

NO_2	**station type**	**No of stations/ pairs**	**Obs. (µg m^{-3})**	**Sim. (µg m^{-3})**	**MFE (%)**	**MFB (%)**	**RMSE (µg m^{-3})**	**FAC2 (%)**
summer	Urban	4/ 2747	19.5	13.5	22	-9	22.6	40
	Traffic	4/ 2964	59.6	44.0	24	-9	46.1	50
winter	Urban	4/ 2292	26.0	14.3	95	-72	23.1	35
	Traffic	4/ 2555	51.6	41.4	41	-11	34.2	59

Table 4.2. *As in Table 4.1 but for PM2.5*

$PM_{2.5}$	**station type**	**No of stations/ pairs**	**Obs. (µg m^{-3})**	**Sim. (µg m^{-3})**	**MFE (%)**	**MFB (%)**	**RMSE (µg m^{-3})**	**FAC2 (%)**
summer	Urban	1/ 699	12.6	15.3	30	20	5.8	96
	Traffic	2/ 1476	15.0	15.1	9	0	6.5	94
winter	-							
	Traffic	2/ 1438	23.1	17.6	67	-30	23.5	72

RI-URBANS (www.RIURBANS.eu) is supported by the European Commission under the Horizon 2020 – Research and Innovation Framework Programme, H2020-GD-2020, Grant Agreement number: 101036245

4.2 Variability within 1 km x 1km areas

EPISODE-CityChem produces two sets of concentration outputs: in 1000m and in 100m resolution. It is noted that 1000m data are not the aggregated 100m concentration values, rather than 100m data base on 1000m outputs, but are further optimized by the street canyon and high-resolution photochemistry mechanisms, analytically described in (Karl et al., 2019).

The normalised standard deviation (NSD), normalised max and min (Nmax and Nmin) are used to investigate the subgrid variability of NO_2 and $PM_{2.5}$ in Athens. The NSD gives information about the variability of the concentrations at the local scale and the Nmax, Nmin quantify the range of local-scale concentrations within a (coarse) grid.

NSD of NO_2 is high in areas/coarse cells of 'low' air pollution in proximity to highways (Figure 4.2, e.g. the National Road at the borders of the urban centre in the North). Inversely, the dense road network in the inner-city centre creates a more homogeneous pattern with high NO2 values, thus concentration variability is smoothed. $PM_{2.5}$ has lower NSD than NO_2 which is expected given the multitude of (area) sources affecting this pollutant, which creates a more homogeneous spatial pattern of its concentrations, with less hyper-local (e.g. road network) dependencies. The spatial pattern is also different (from this for NO_2), following that of concentrations, which are elevated in the urbanized area of the inner-city centre. Winter and summer values and spatial variability of NSD are similar for both pollutants.

The local-scale concentrations tend to be higher than the regional, the closer to the inner-city centre (Figure 4.3). In particular, NO_2 concentrations at the 100m are double-triple than the 1000m ones over the city centre, while they can be up to 15 times higher than the 1000m ones over the road network during summertime, when photochemistry is enhanced. $PM_{2.5}$ local-scale (100m cell) concentrations are up to 2 times higher than regional values (1000m cell) and the spatial field of Nmax is more extended during wintertime, when residential biomass emissions are high. Low concentrations are also affected by grid resolution (Figure 4.4). Sub-grid minima for NO_2 are lower than 0.1 times the regional NO2 values, especially during the warm period. $PM_{2.5}$ differences are higher than 0.6, given the 'less local' character of this pollutant.

Overall (Table 4.3), the subgrid variability and value ranges for Athens urban centre are found higher for NO_2 than $PM_{2.5}$.

RI-URBANS (www.RIURBANS.eu) is supported by the European Commission under the Horizon 2020 – Research and Innovation Framework Programme, H2020-GD-2020, Grant Agreement number: 101036245

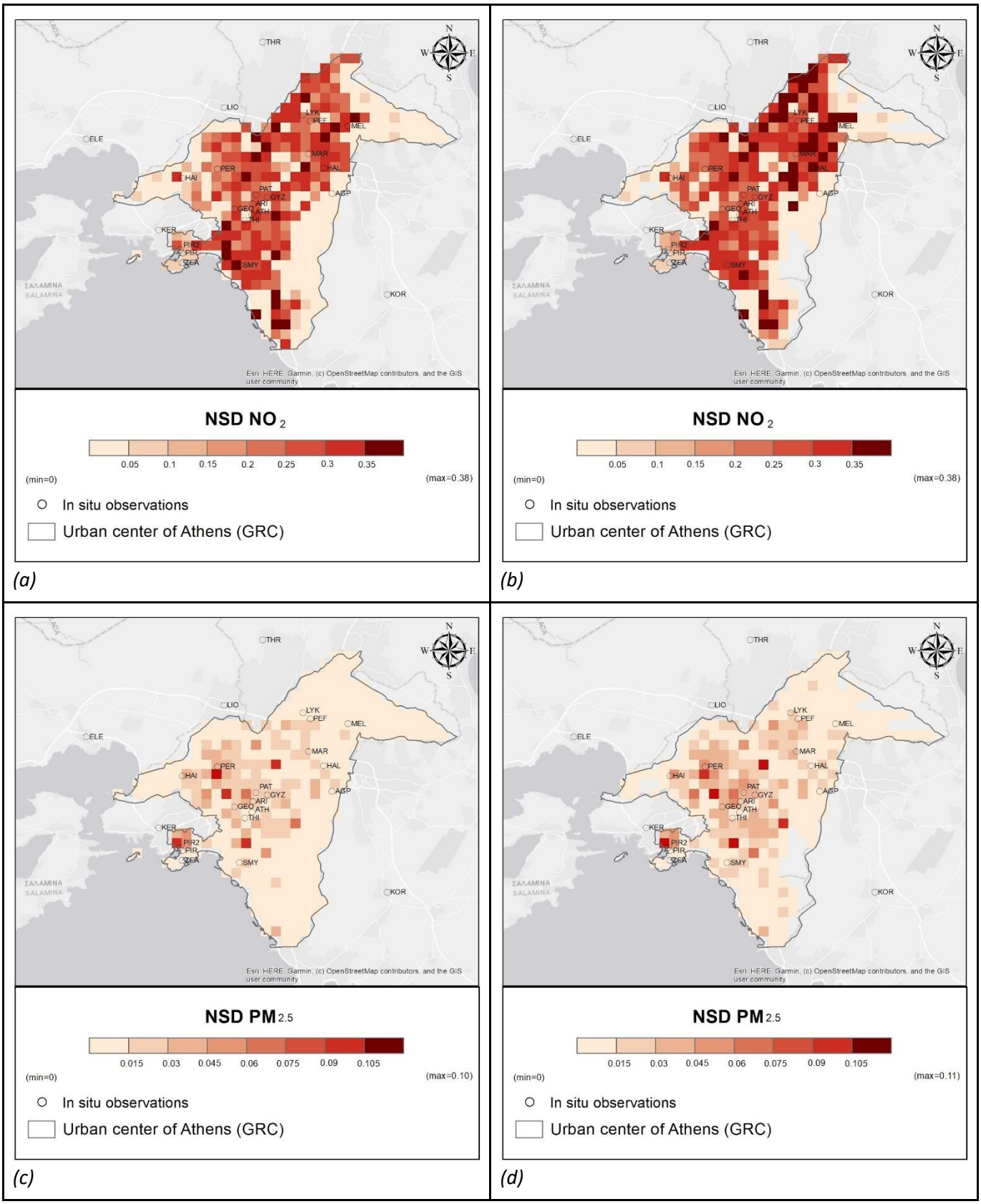

Figure 4.2. *NSD of NO_2 [(a) and (b)] and $PM_{2.5}$ [(c) and (d)], for summer (left panels) and winter (right panels) in Athens, using EPISODE-CityChem.*

RI-URBANS (www.RIURBANS.eu) is supported by the European Commission under the Horizon 2020 – Research and Innovation Framework Programme, H2020-GD-2020, Grant Agreement number: 101036245

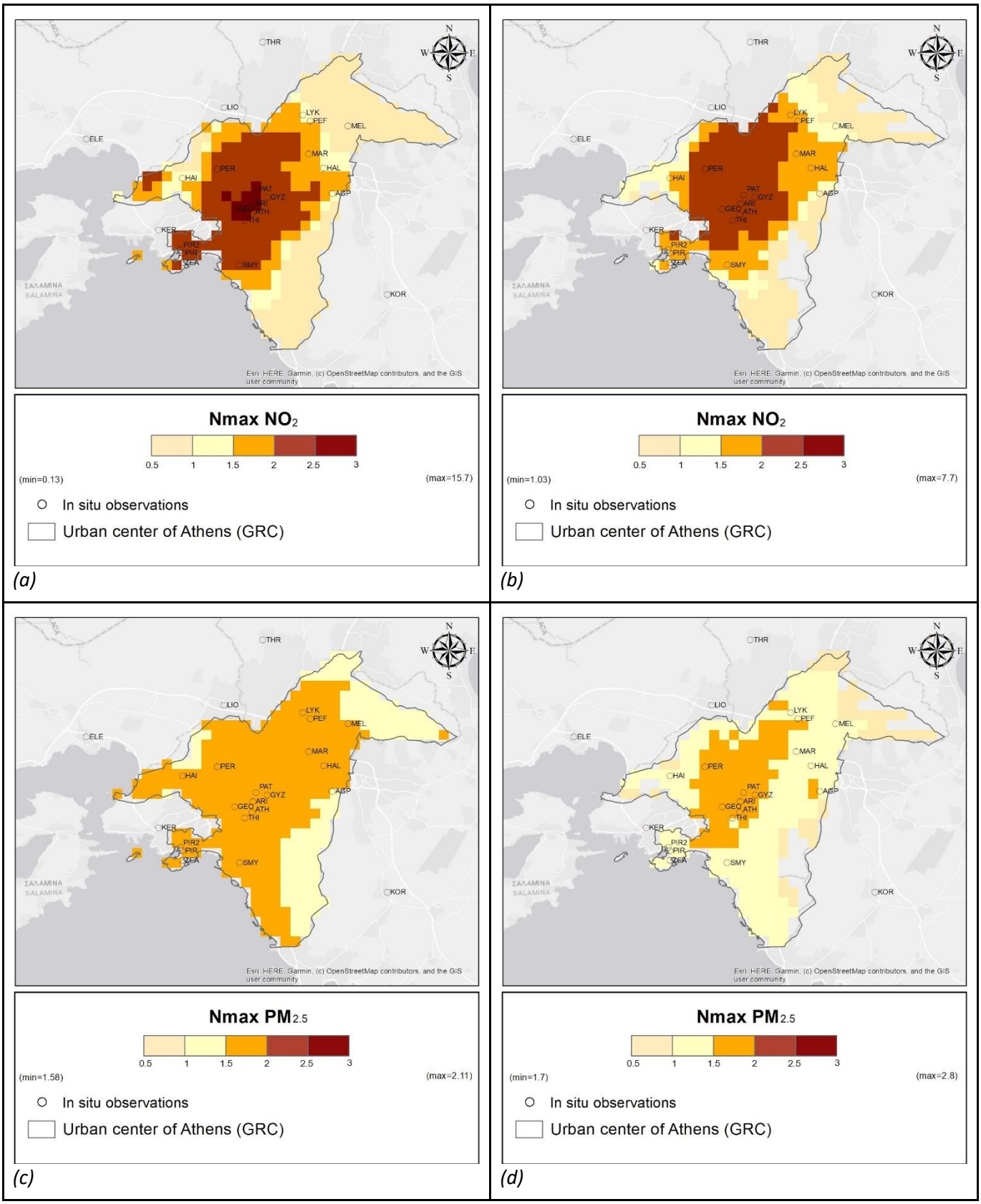

Figure 4.3. *As in Figure 4.2, but for Nmax.*

RI-URBANS (www.RIURBANS.eu) is supported by the European Commission under the Horizon 2020 – Research and Innovation Framework Programme, H2020-GD-2020, Grant Agreement number: 101036245

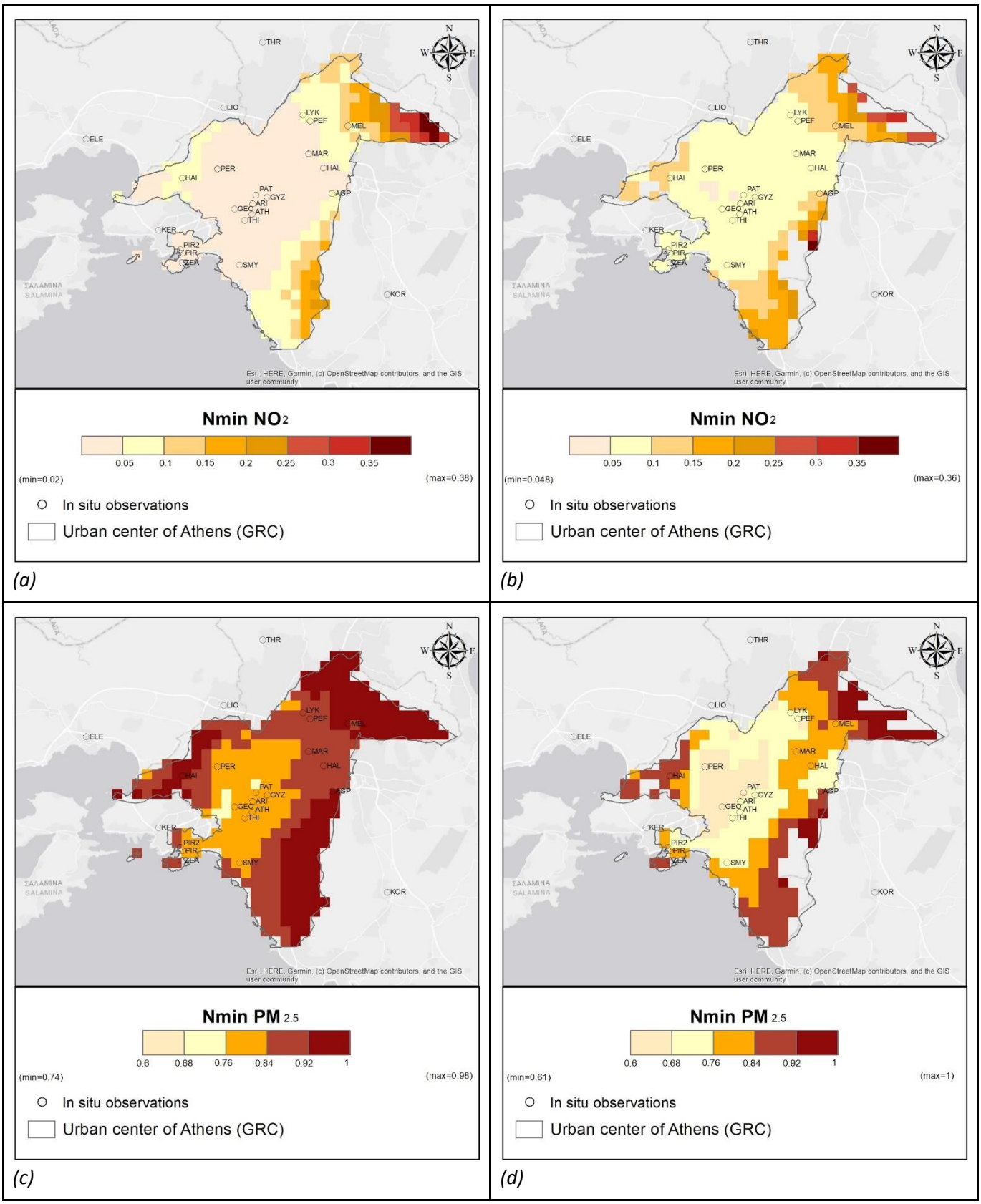

***Figure 4.4**. As in Figure 4.2, but for Nmin.*

RI-URBANS (www.RIURBANS.eu) is supported by the European Commission under the Horizon 2020 – Research and Innovation Framework Programme, H2020-GD-2020, Grant Agreement number: 101036245

Table 4.3. *Domain averaged NSD of NO_2 and $PM_{2.5}$ in Athens urban center for summer and winter.*

Athens	*NSD*		*Nmin, Nmax*	
	NO_2	*$PM_{2.5}$*	*NO_2*	*$PM_{2.5}$*
summer	*0.16*	*0.01*	*0.07, 4.3*	*0.9, 3.0*
winter	*0.19*	*0.01*	*0.1, 2.1*	*0.8, 2.8*

4.3 Variability of population exposure and of exposure scaling factor

The population-weighted concentration (PWC) per season is an equivalent to the UN SDG 11.6.2 indicator, which (slightly) modifies concentrations in spatially aggregated areas (here, 1 km cells), using the high resolution (here, residential) population density, as a weighting factor to the high-resolution concentrations (here, 100 m cells). Such a mapping (Figure 4.5) is more useful for health-related studies, as it represents population exposure to the studied pollutant.

RI-URBANS (www.RIURBANS.eu) is supported by the European Commission under the Horizon 2020 – Research and Innovation Framework Programme, H2020-GD-2020, Grant Agreement number: 101036245

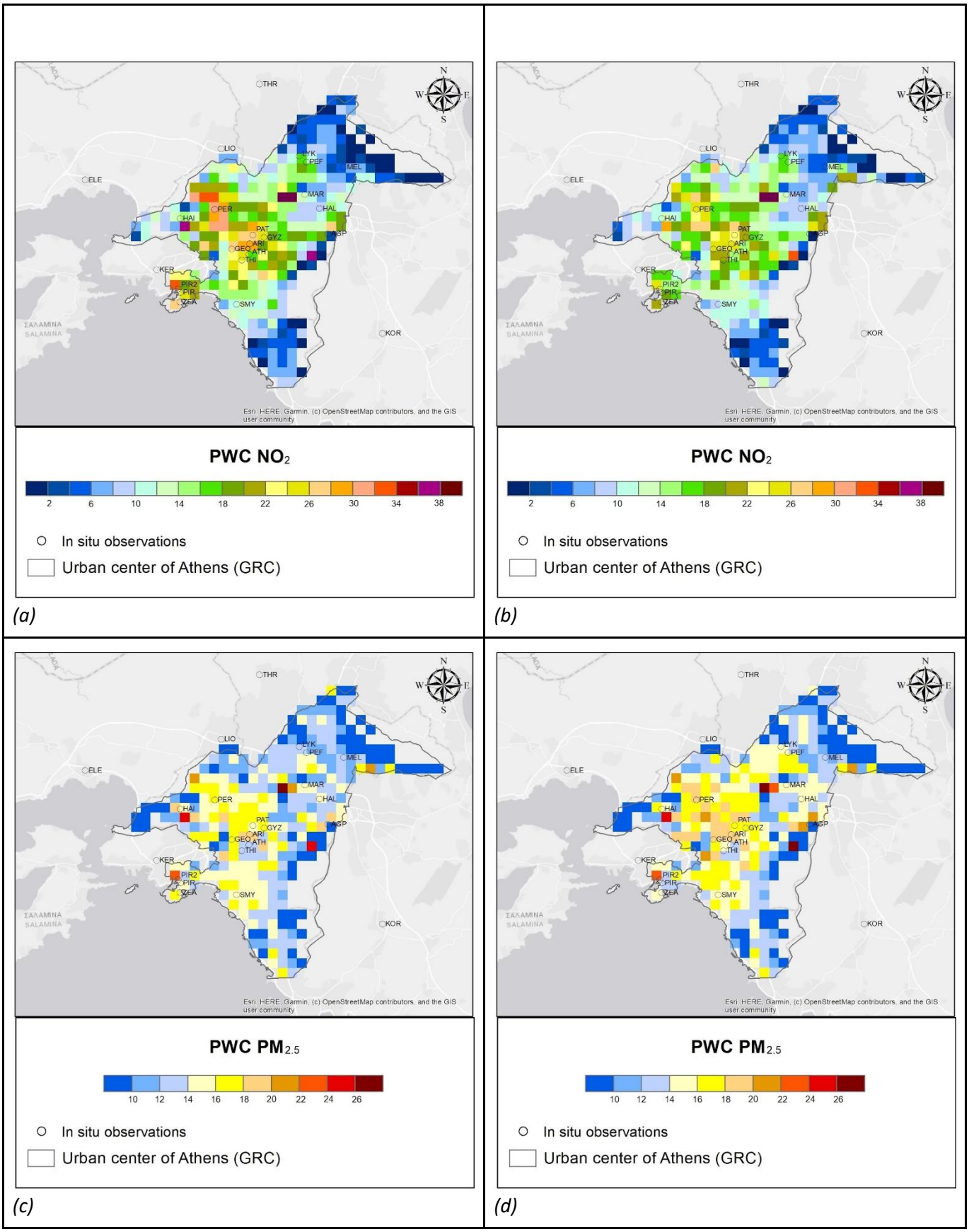

Figure 4.5. *PWC (μg m^{-3}) of NO_2[(a) and (b)] and $PM_{2.5}$ [(c) and (d)] in summer (left panels) and winter (right panels) over the urban center of Athens.*

RI-URBANS (www.RIURBANS.eu) is supported by the European Commission under the Horizon 2020 – Research and Innovation Framework Programme, H2020-GD-2020, Grant Agreement number: 101036245

PWC is here used to estimate the mapping of the exposure scaling factor (ESF, Figure 4.6). As shown for NO_2, ESF is less than unity in most areas. To explore whether this is due to a negative correlation between the sub-grid population and concentrations or to a negative sub-grid bias, coarse (1 km) maps of near-road concentrations (μg m^{-3}) over Athens for summer and winter were prepared (not shown here). Comparisons of these maps and Figure 4.1 along with their NMB mapping revealed that coarse representation of NO_2 gives higher values than high-resolution model outputs. This can be explained by the fact that on road emissions are homogeneously dispersed over a coarser cell, rather than the on road 100m cells. This resulted in overestimated concentrations over the non-road areas. Thus, ESF lower than 1 indicates a negative sub-grid bias for NO_2, using the EPISODE-CityChem modelling tool for Athens. It should be reminded that the road network of Athens urban centre is quite dense, thus most (coarse) grid cells are affected by local traffic.

For $PM_{2.5}$, there is an area with ESF values larger than unity, which is explained by the fact that sub-grid population is positively correlated with the sub-grid concentrations. This is further suggesting that the regional $PM_{2.5}$ predictions underestimate the intra-urban population exposure of Athens. Nevertheless, ESF values at the road cells remain below unity as in NO_2, which is again due to a negative sub-grid bias for the on-road cells.

RI-URBANS (www.RIURBANS.eu) is supported by the European Commission under the Horizon 2020 – Research and Innovation Framework Programme, H2020-GD-2020, Grant Agreement number: 101036245

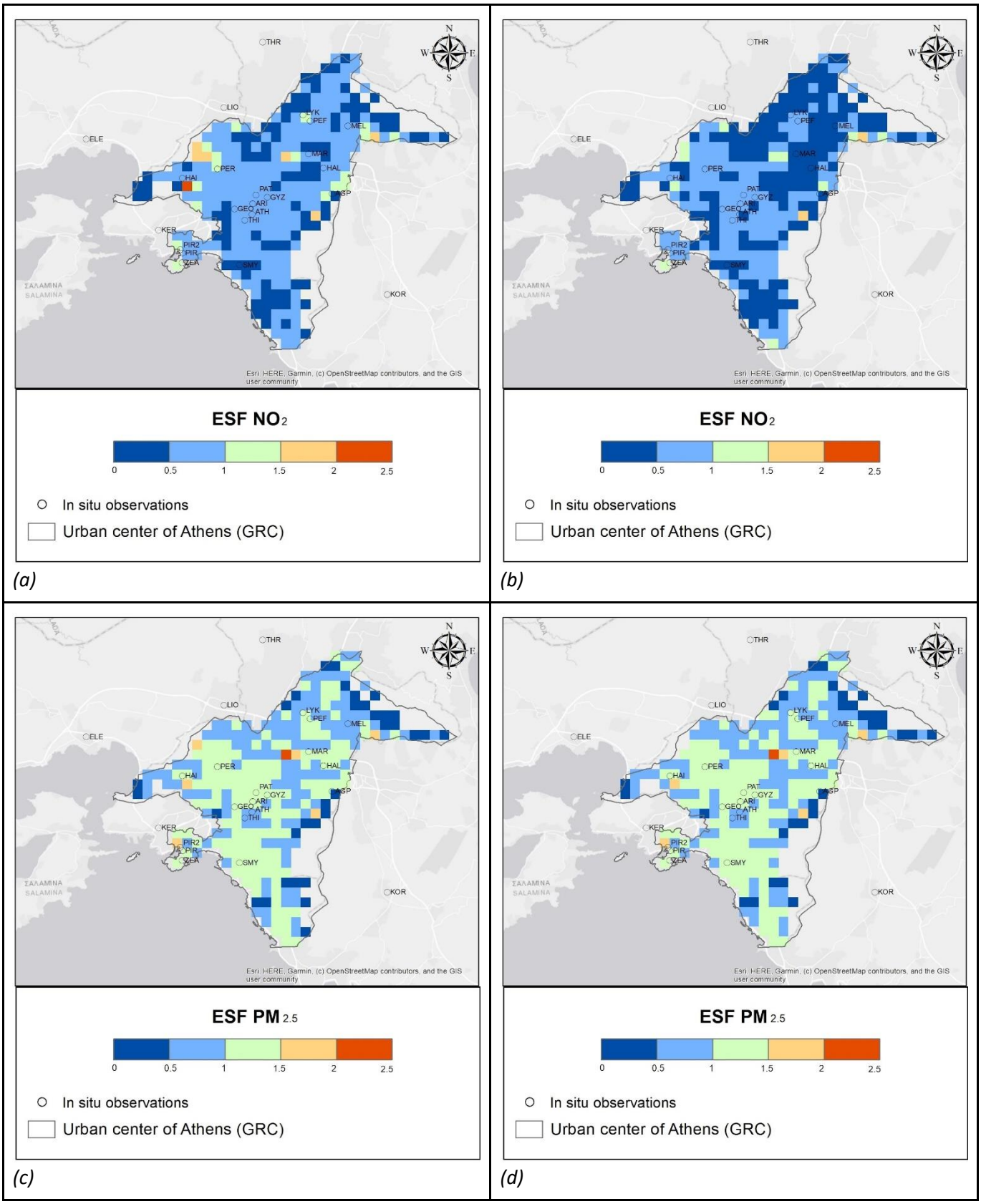

Figure 4.6. *as in Figure 4.5, but for ESF.*

RI-URBANS (www.RIURBANS.eu) is supported by the European Commission under the Horizon 2020 – Research and Innovation Framework Programme, H2020-GD-2020, Grant Agreement number: 101036245

Domain (here, urban centre)-averaged values (Table 4.4) for PWC in winter and summer are close, though -as expected- they are higher in summer for NO_2 and in winter for $PM_{2.5}$ (see more in Section 4.1). The ESF does not change between seasons, and it indicates that when an aggregated (here, for the urban centre of the city) value of $PM_{2.5}$ is requested, then 1km resolution simulations are equally competent to represent this value, as population-weighted predictions from high-resolution CTM applications. On the contrary, regional-scale NO_2 outputs overestimate population exposure.

Table 4.4. *Domain averaged PWC and ESF of NO_2 and $PM_{2.5}$ in Athens urban centre for summer and winter.*

Athens	*PWC (µg m-3)*		*ESF*	
	NO_2	*$PM_{2.5}$*	*NO_2*	*$PM_{2.5}$*
summer	*14.1*	*13.6*	*0.7*	*1*
winter	*13*	*14.1*	*0.6*	*1*

4.4 Variability between pollutants

The variability between NO_2 and $PM_{2.5}$ is reflected by their ratio for summer and winter (Figure 4.7). Different colours indicate a quantile division of this ratio, which means that each of these 4 colours represents an equal number of 100m x 100m grids. As expected, higher values of $NO_2/PM_{2.5}$ are predicted mainly over the road network. Lower values occur where residential combustion emissions occur. The spatial plots of the ratio do not differ significantly between summer and winter, although values are lower over residential areas during wintertime (higher $PM_{2.5}$ values).

RI-URBANS (www.RIURBANS.eu) is supported by the European Commission under the Horizon 2020 – Research and Innovation Framework Programme, H2020-GD-2020, Grant Agreement number: 101036245

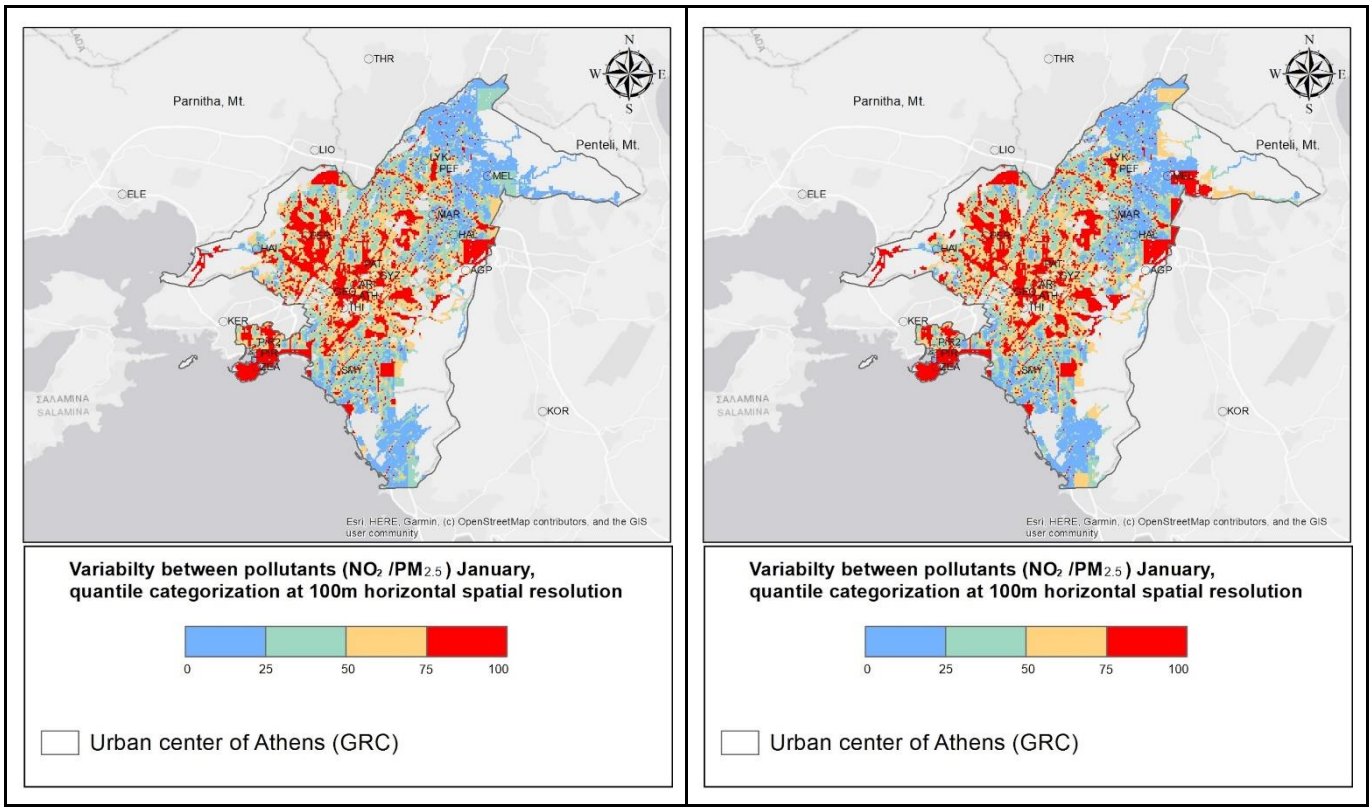

Figure 4.7. *Ratio between predicted NO_2 and $PM_{2.5}$ concentrations for summer (left panel) and winter (right panel) in Athens, using EPISODE-CityChem.*

5. Rotterdam Pilot

The main analyses in Rotterdam are based on a mobile monitoring campaign, performed with a car measuring UFP, NO_2 and BC. Also, *measurements by cyclists or* pedestrians with portable instruments for BC are performed. In both campaigns, large spatial gradients were observed. For BC, we compare the car measurements and models to the measurements and models of the bikes. Furthermore, we compare the car models for BC to a local dispersion model (CIMLK) and compare values to five reference measurement stations.

Rotterdam is the second biggest city in the Netherlands and has a large harbour as the main source of pollution. The car fleet in the Netherlands is 80% petrol, 14% diesel and 5% hybrid and electric.

5.1 Car Measurements

We used a car to measure the ambient concentrations of NO_2, BC and UFP during two seasons; one in November-December 2022 and in May-July 2023. The car was equipped with lab-grade 1 Hz NO_2 (CAPS, Aerodyne Research Inc., USA), 1 Hz BC (AE33, Magee Scientific), and 1 Hz UFP (EPC 3783, TSI) monitors measuring simultaneously. A Global Positioning System (GPS) (G-Star IV, GlobalSat, Taiwan) was used to record the location of the car, which was linked to the measuring equipment via date and time. The measurements were mainly carried out between 08.00 to 22.00 hours every day in the study period (including some weekend days) in different parts of the city. The aim was to reduce possible space and time autocorrelation. Therefore, there is no need to temporally correct the measurements.

The data was winsorised to the 2.5th and the 97.5th percentile. That is, measured concentration levels below the 2.5th percentile and above the 97.5th percentile were “replaced” by the respective percentile values (Kerckhoffs

RI-URBANS (www.RIURBANS.eu) is supported by the European Commission under the Horizon 2020 – Research and Innovation Framework Programme, H2020-GD-2020, Grant Agreement number: 101036245

et al. 2022). This procedure is done to balance the unduly influence of extreme values, while allowing very high pollution values. For averaging, the data was first assigned to the nearest street and aggregated over each 50-meter (min: 30m and max: 60m) street segment per individual drive day. In total xx street segments were measured.

For the maps, we used linear mixed-effect models. These models use fixed effects estimated based on determinants from a linear regression model (SLR) and random intercepts for all individual street segments (random-effect model). Such a model combines the advantages of "data-only" mapping and LUR modelling, meaning that all individual measurements can influence the output of the fixed-effect model based on the measured between and within-street segment concentration variation. The mixed-effect modelling framework has been extensively explained and validated, demonstrating the feasibility of the adopted approach to develop high-resolution NO_2 concentration maps for Amsterdam and Copenhagen with better performance than data-only and LUR-only approaches.

5.2 Local Pollution Maps

Spatial patterns are highlighted in Figures 5.1 to 5.3. As expected, the major roads in and around Rotterdam have the highest concentrations of air pollution. For UFP, this is more pronounced on the highways than for the other two pollutants. UFPs quickly transform through physicochemical processes, like coagulation or condensation and can reach background levels within 300 metres of a highway, with even sharper gradients for the smaller particles. For NO_2 and BC, elevated concentrations are mainly found towards the city centre.

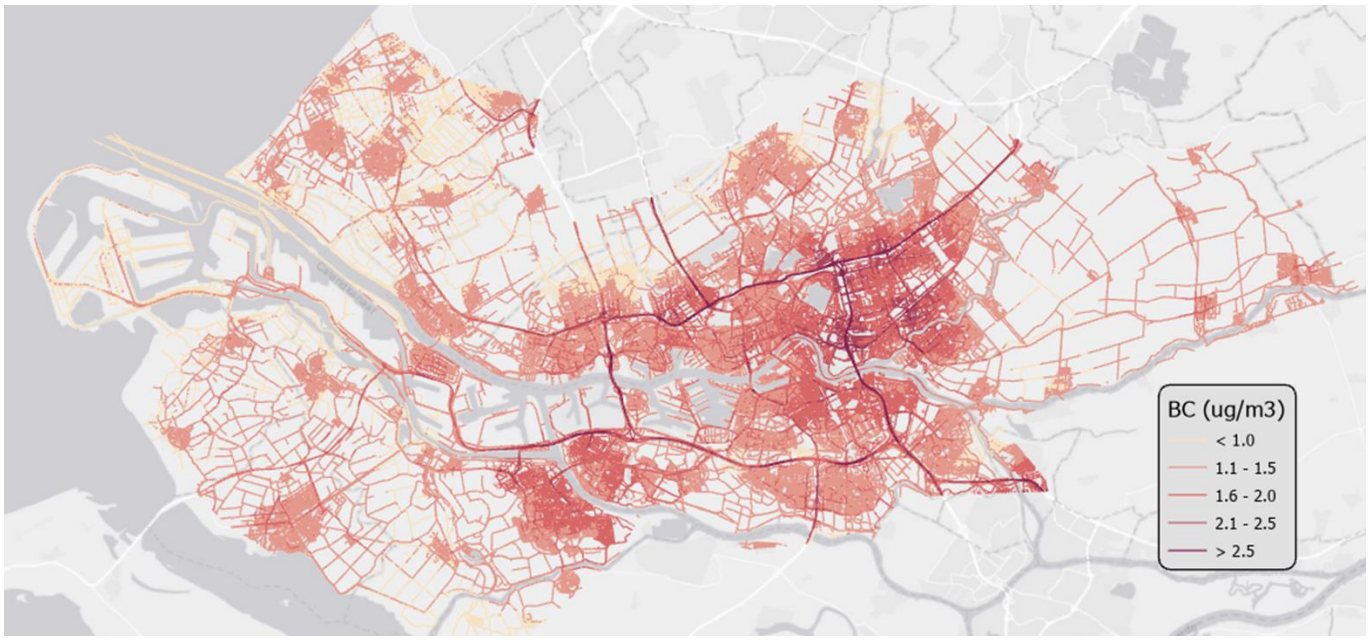

Figure 5.1. *Mixed-effect model predictions for BC concentration levels in Rotterdam.*

RI-URBANS (www.RIURBANS.eu) is supported by the European Commission under the Horizon 2020 – Research and Innovation Framework Programme, H2020-GD-2020, Grant Agreement number: 101036245

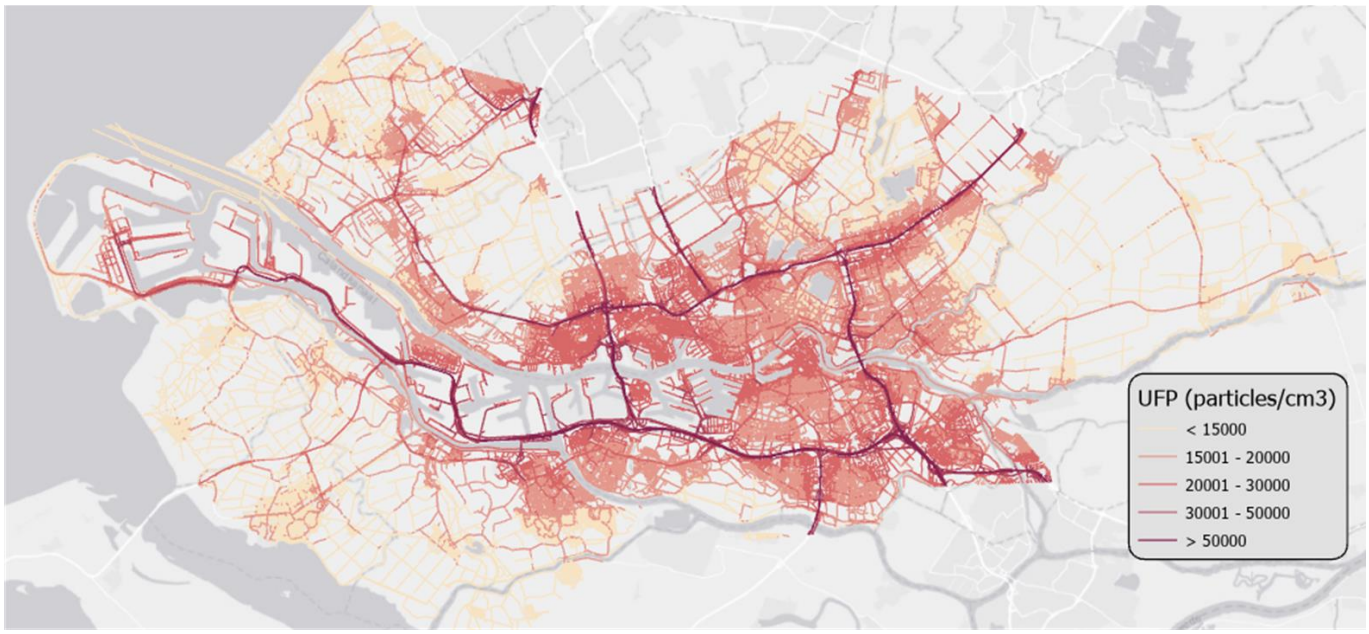

Figure 5.2. *Mixed-effect model predictions for UFP concentration levels in Rotterdam.*

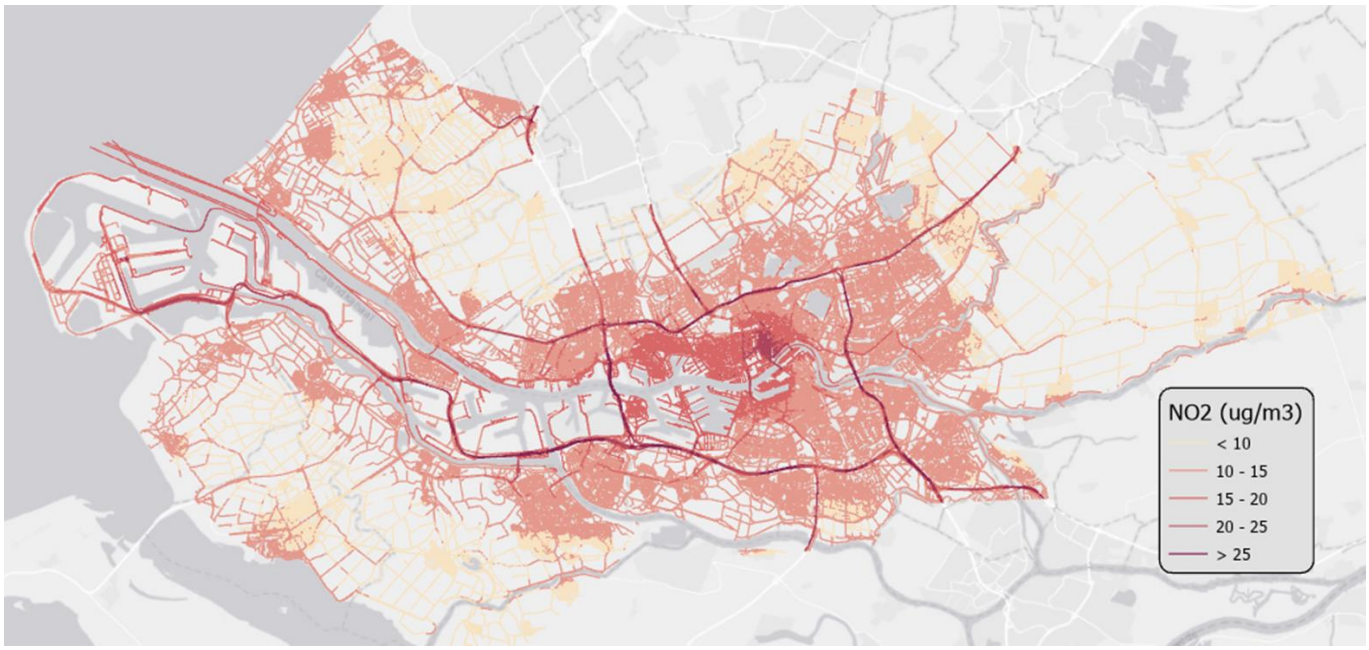

Figure 5.3. *Mixed-effect model predictions for NO_2 concentration levels in Rotterdam.*

5.3 Ratio Analysis

We also show ratios between pollutants in Figures 5.4 to 5.6. They are based on a quantile division of predictions of two pollutants and their relative loading. So, each of the four colours in the 2x2 box represent an equal number of road segments. High NO_2 concentrations are more restricted to the city centre, UFP is most pronounced on the major roads and BC is relatively elevated in the suburbs.

RI-URBANS (www.RIURBANS.eu) is supported by the European Commission under the Horizon 2020 – Research and Innovation Framework Programme, H2020-GD-2020, Grant Agreement number: 101036245

Figure 5.4. *Ratio between predicted* NO_2 *concentrations and UFP concentrations in Rotterdam. Each of the four colours in the 2x2 box represent an equal number of road segments.*

Figure 5.5. *Ratio between predicted* NO_2 *concentrations and BC concentrations in Rotterdam. Each of the four colours in the 2x2 box represent an equal number of road segments.*

RI-URBANS (www.RIURBANS.eu) is supported by the European Commission under the Horizon 2020 – Research and Innovation Framework Programme, H2020-GD-2020, Grant Agreement number: 101036245

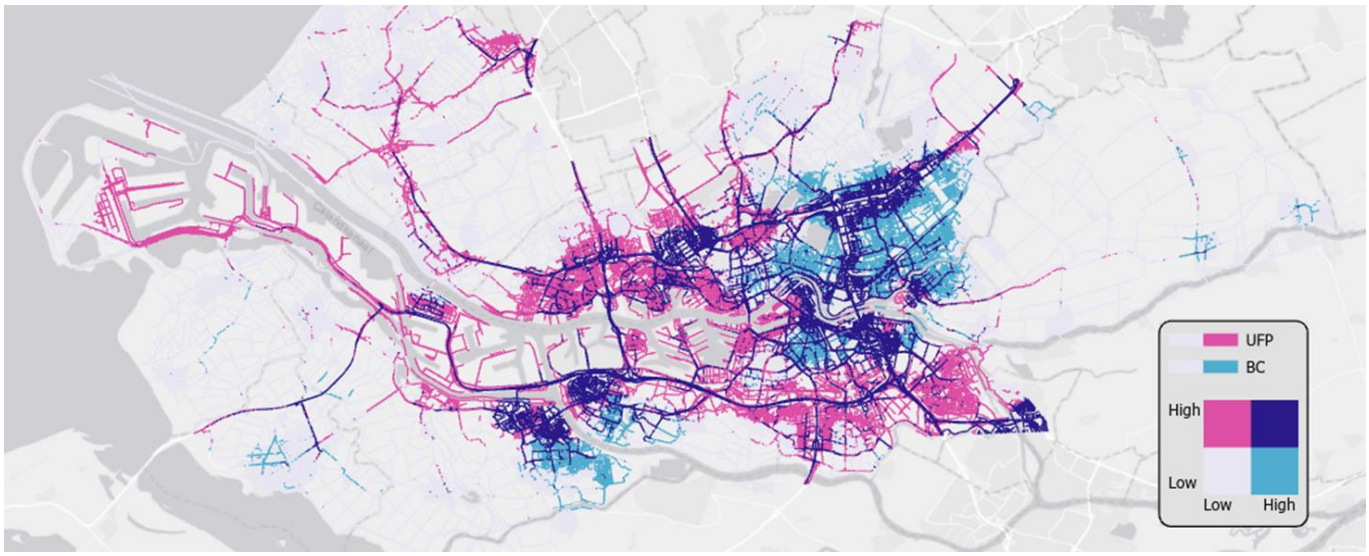

Figure 5.6. *Ratio between predicted UFP concentrations and BC concentrations in Rotterdam. Each of the four colours in the 2x2 box represent an equal number of road segments.*

5.4 Comparison of Car model with other data sources

5.4.1 Bikes

Bike measurements were done by employees of DCMR (local environmental agency) and the city of Rotterdam, while travelling from and to their work. The coverage of the measurements is shown below.

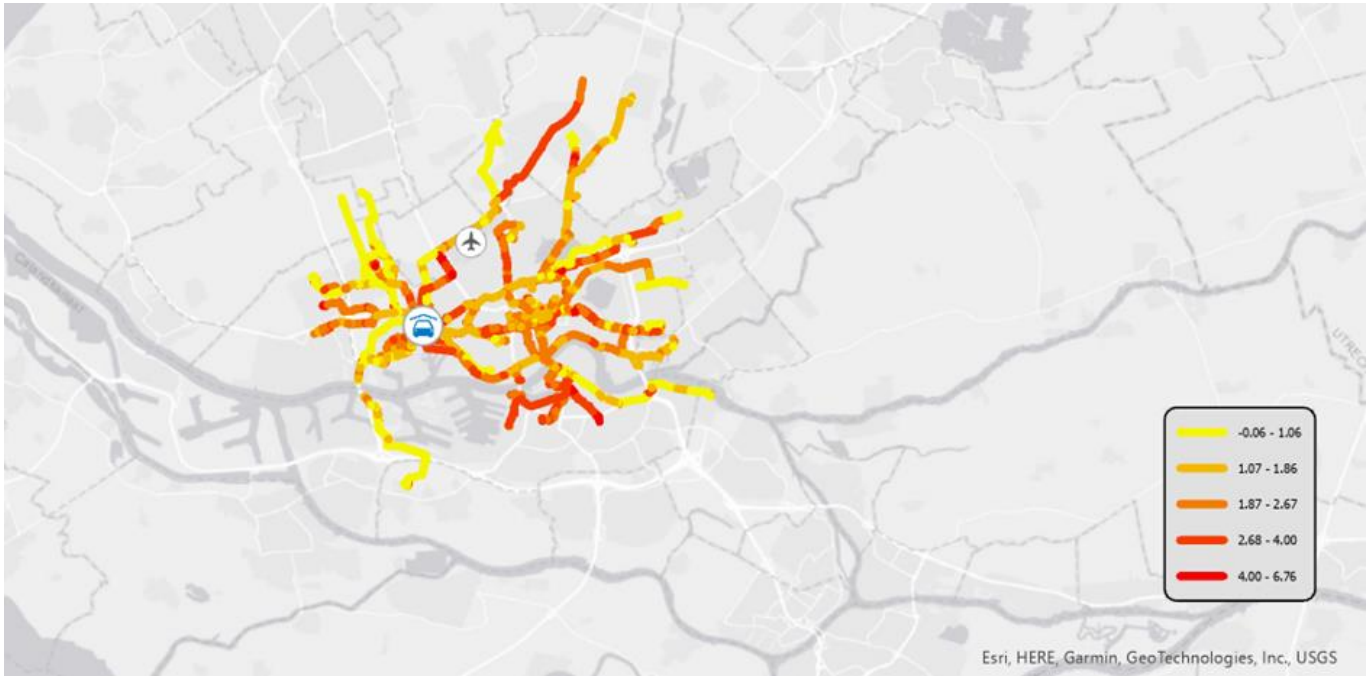

Figure 5.7. *Coverage and BC concentrations of all bike measurements.*

RI-URBANS (www.RIURBANS.eu) is supported by the European Commission under the Horizon 2020 – Research and Innovation Framework Programme, H2020-GD-2020, Grant Agreement number: 101036245

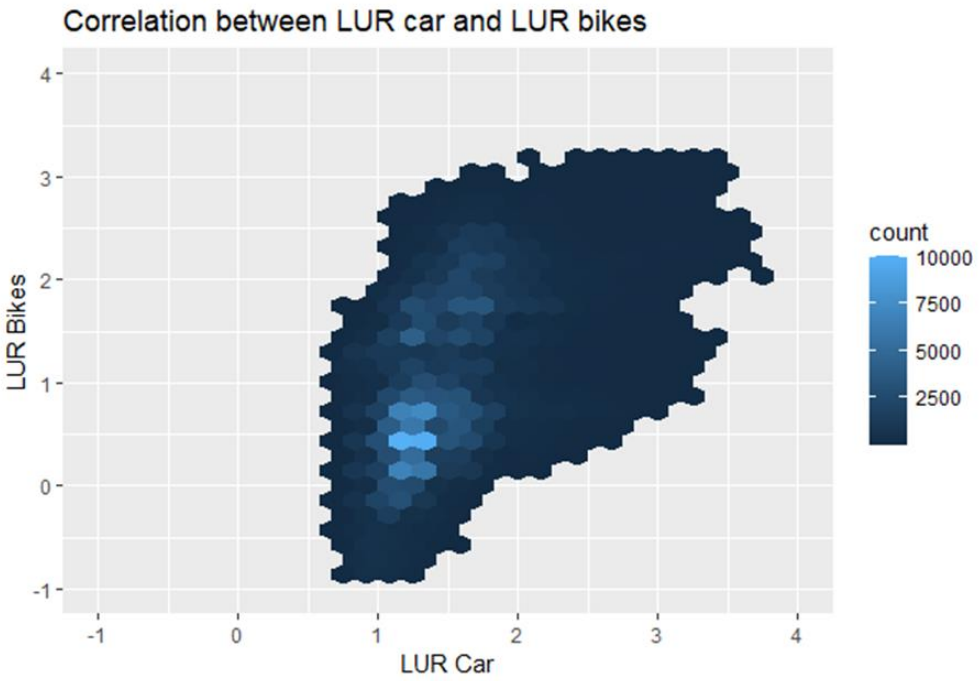

Figure 5.8. *Comparison of predicted BC concentrations by the Car and Bikes.*

5.4.2 CIMLK

The CIMLK (Centraal Instrument Monitoring Luchtkwaliteit) is a tool from the government that monitors the air quality in the Netherlands. Therefore, a dispersion model is used to calculate the BC concentrations on every major road with 100m intervals on both sides of the road, example below. The total number of roads with CIMLK predictions is around 35.000.

Figure 5.9: *Example of the spatial distribution of CIMLK monitoring points.*

The correlation between the CIMLK and the model based on the car measurements is 0.64. For the predictions based on the bike measurements, this is 0.55. Notably, the predictions by the CIMLK model do not exceed 1 ug/m3, while the car model predicts concentrations up to 3.5 ug/m3. One factor that should be taken into account here is that the car model measures and therefore predicts concentrations on the middle of the road, whereas the CIMNLK model predicts concentrations on the side of the road.

RI-URBANS (www.RIURBANS.eu) is supported by the European Commission under the Horizon 2020 – Research and Innovation Framework Programme, H2020-GD-2020, Grant Agreement number: 101036245

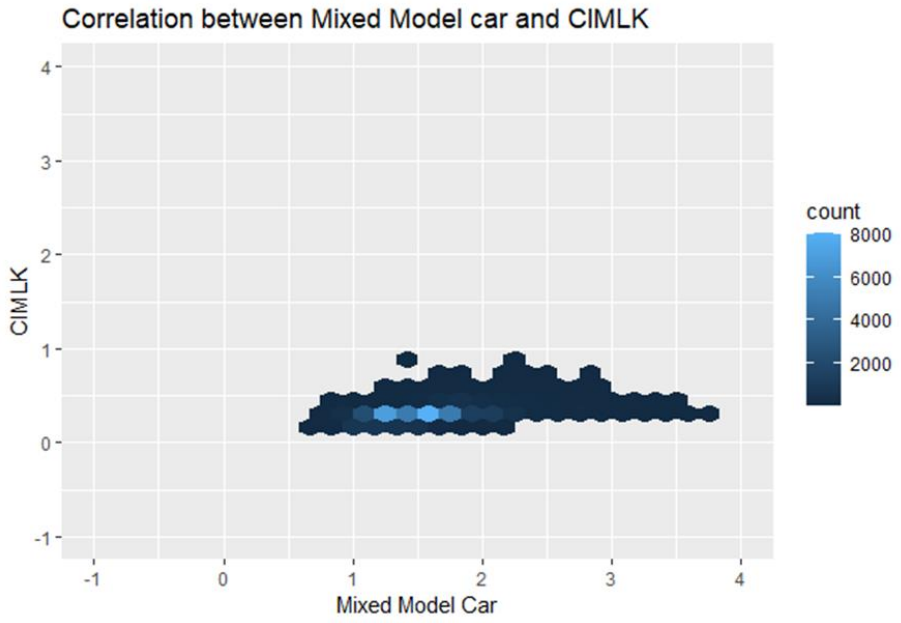

Figure 5.10. *Comparison of predicted BC concentrations by the Car and CIMLK.*

5.4.3 LML

The LML is a network of official measurement sites in the Netherlands, operated by the Dutch Environmental Agency. They measure BC concentrations at five different locations in Rotterdam.

The correlation between the CIMLK and the model based on the car measurements is 0.4. Notably, the measurements from the LML do exceed 1 ug/m3, while this was not the case for the CIMLK predictions.

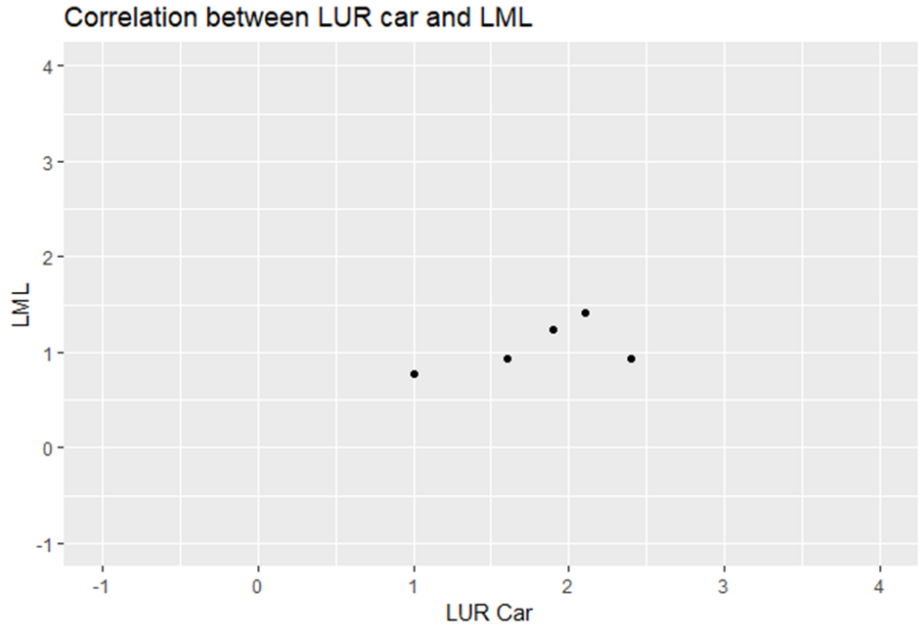

Figure 5.11. *Comparison between predicted BC concentrations by the Car reference site measurements by LML.*

RI-URBANS (www.RIURBANS.eu) is supported by the European Commission under the Horizon 2020 – Research and Innovation Framework Programme, H2020-GD-2020, Grant Agreement number: 101036245

5.5 Seasonal Differences

5.5.1 BC

Concentrations of BC in Rotterdam pilot are described in Table 5.1. The BC concentrations were on average twice as high in Winter, compared to the Summer measurements, respectively 1,91 ug/m^3 and 0.95 ug/m^3. Correlation between the Summer and Winter model based on all streets in Rotterdam is 0.79. The higher BC concentrations in the Winter can potentially be attributed by wood smoke, as elevated concentrations are seen in the suburbs as well.

Table 5.1. *Statistics of BC concentrations with different methods in Rotterdam in Winter and Summer.*

BC_Data	BC_LUR	BC_LUR_Winter	BC_LUR_Summer	BC_Mixed
Min. : 0.00	Min. :0.700	Min. :0.70	Min. :0.3000	Min. :0.700
1st Qu.: 0.70	1st Qu.:1.200	1st Qu.:1.40	1st Qu.:0.7000	1st Qu.:1.200
Median : 1.30	Median :1.400	Median :1.70	Median :0.7000	Median :1.400
Mean : 1.56	Mean :1.418	Mean :1.76	Mean :0.7857	Mean :1.418
3rd Qu.: 2.00	3rd Qu.:1.600	3rd Qu.:2.10	3rd Qu.:0.9000	3rd Qu.:1.600
Max. :11.90	Max. :3.700	Max. :4.30	Max. :2.4000	Max. :4.000

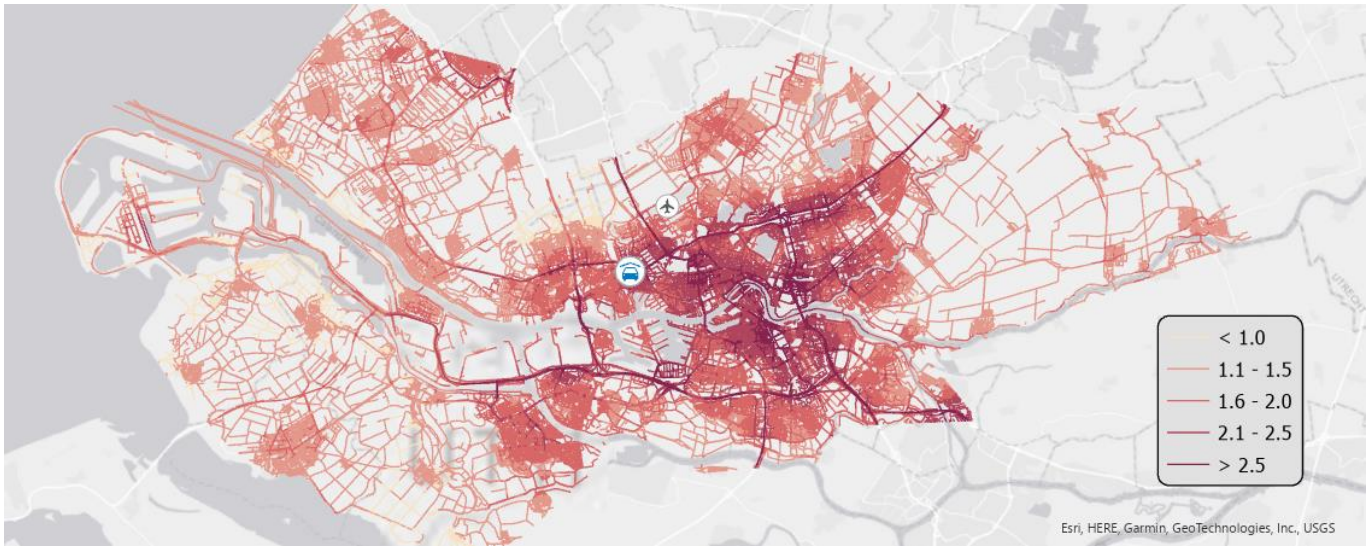

Figure 5.12. *Winter LUR model BC.*

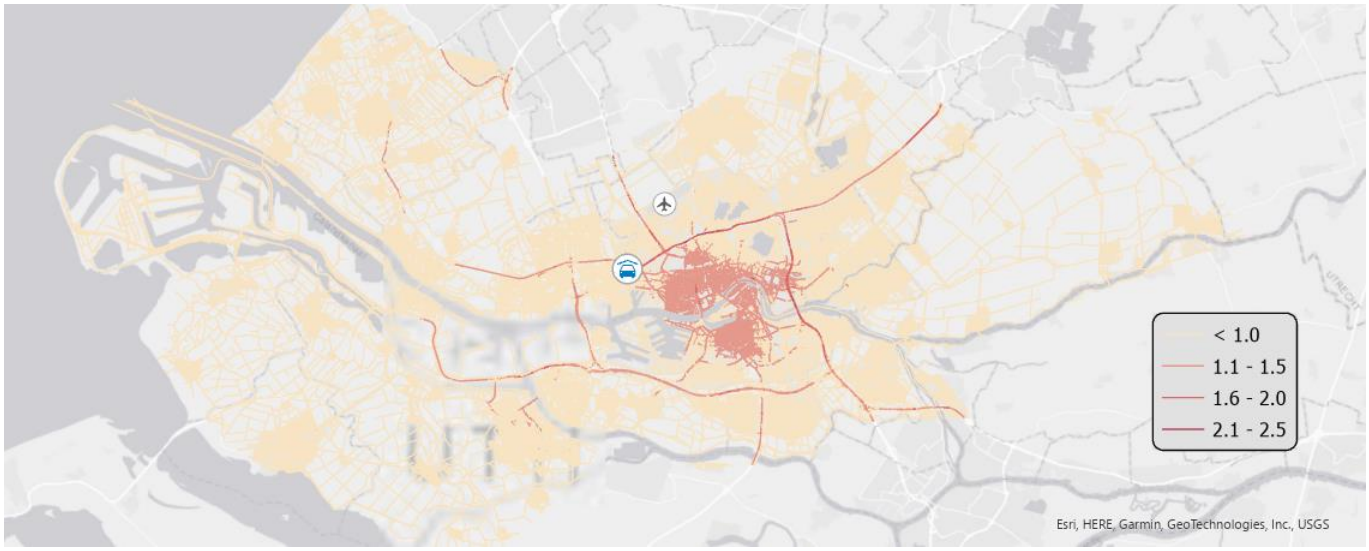

Figure 5.13. *Summer LUR model BC.*

RI-URBANS (www.RIURBANS.eu) is supported by the European Commission under the Horizon 2020 – Research and Innovation Framework Programme, H2020-GD-2020, Grant Agreement number: 101036245

5.5.2 UFP

Concentrations of UFP in Rotterdam are presented in Table 5.2. The concentrations were on average slightly higher in Summer, compared to the Winter measurements, respectively 23.000 p/cm^3 and 20.000 p/cm^3. Correlation between the Summer and Winter model based on all streets in Rotterdam is 0.91. In both campaigns, the highways and major roads account for the biggest variation in pollution. No distinct spatial patterns can be observed between the Summer and Winter model.

Table 5.2. *Statistics of UFP concentrations with different methods in Rotterdam in Winter and Summer.*

UFP_Data	UFP_LUR	UFP_LUR_Winter	UFP_LUR_Summer	UFP_Mixed
Min. : 2400	Min. :11000	Min. : 8765	Min. : 13668	Min. :11000
1st Qu.: 9780	1st Qu.:15100	1st Qu.:15035	1st Qu.: 17341	1st Qu.:15100
Median : 16300	Median :18200	Median :18460	Median : 19722	Median :18200
Mean : 24248	Mean :21044	Mean :20326	Mean : 23269	Mean :21044
3rd Qu.: 30000	3rd Qu.:22800	3rd Qu.:23057	3rd Qu.: 23355	3rd Qu.:22800
Max. :130000	Max. :95600	Max. :78727	Max. :119063	Max. :97800

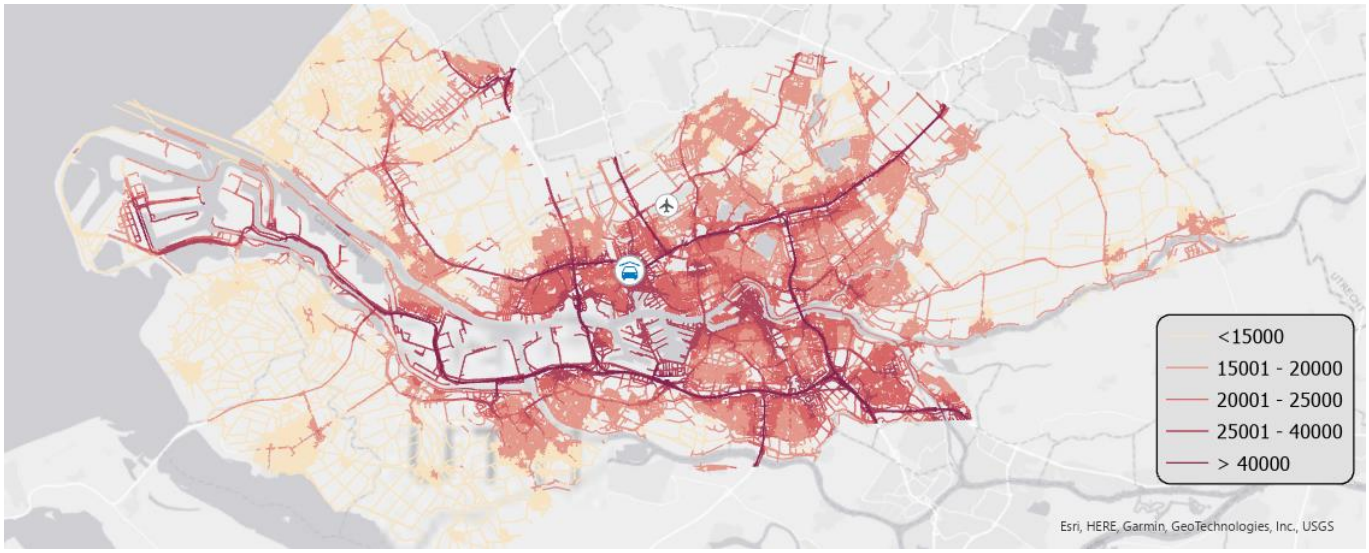

Figure 5.14. *Winter UFP LUR model.*

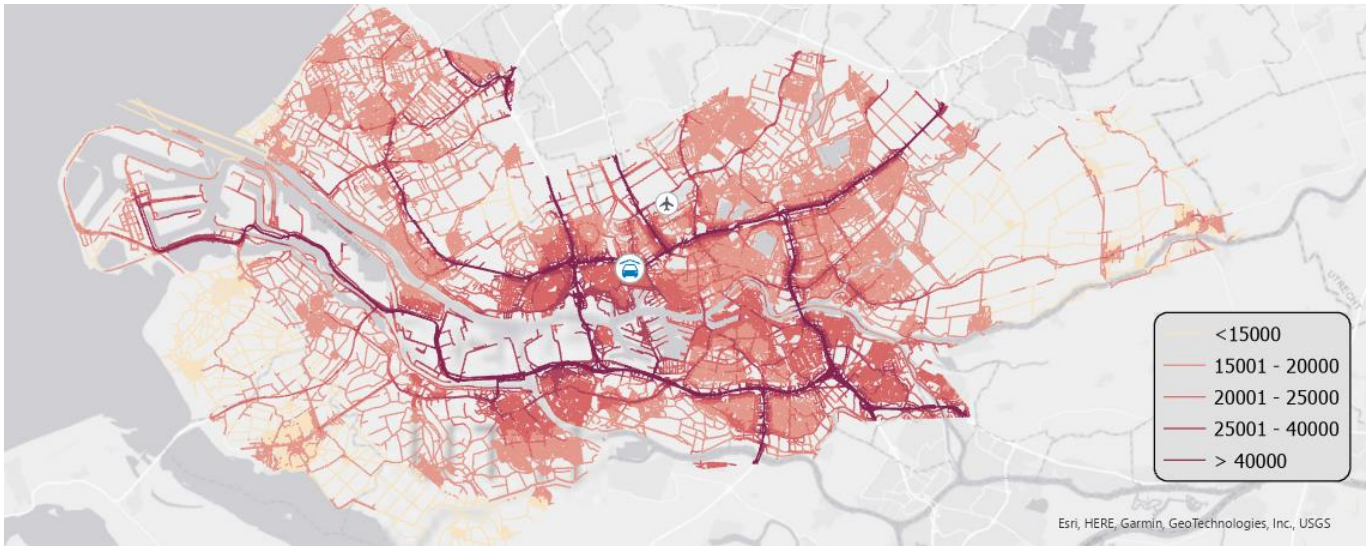

Figure 5.15. *Summer UFP LUR model.*

RI-URBANS (www.RIURBANS.eu) is supported by the European Commission under the Horizon 2020 – Research and Innovation Framework Programme, H2020-GD-2020, Grant Agreement number: 101036245

5.5.3 NO_2

Table 5.3 presents the statistics of NO2 concentrations in Rotterdam during Winter and Summer. Unexpectedly, concentrations were on average slightly higher in Summer, compared to the Winter measurements, respectively 14 ug/m^3 and 12 ug/m^3. Correlation between the Summer and Winter model based on all streets in Rotterdam was 0.76.

NO2_Data	NO2_LUR	NO2_LUR_Winter	NO2_LUR_Summer	NO2_Mixed
Min. : 0.00	Min. : 7.00	Min. : 5.00	Min. : 7.00	Min. : 7.00
1st Qu.: 8.00	1st Qu.:10.00	1st Qu.:10.00	1st Qu.:10.00	1st Qu.:10.00
Median :12.00	Median :12.00	Median :11.00	Median :12.00	Median :12.00
Mean :14.32	Mean :12.85	Mean :11.68	Mean :13.99	Mean :12.85
3rd Qu.:18.00	3rd Qu.:15.00	3rd Qu.:13.00	3rd Qu.:16.00	3rd Qu.:15.00
Max. :87.00	Max. :36.00	Max. :22.00	Max. :58.00	Max. :38.00

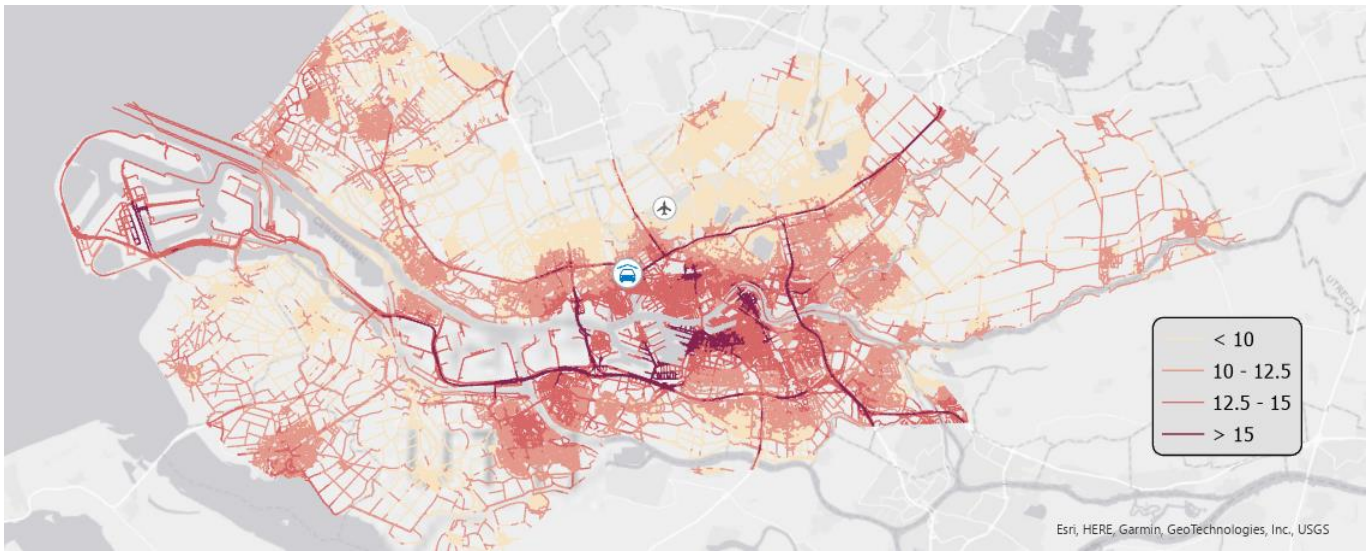

Figure 5.16. *Winter NO_2 LUR model.*

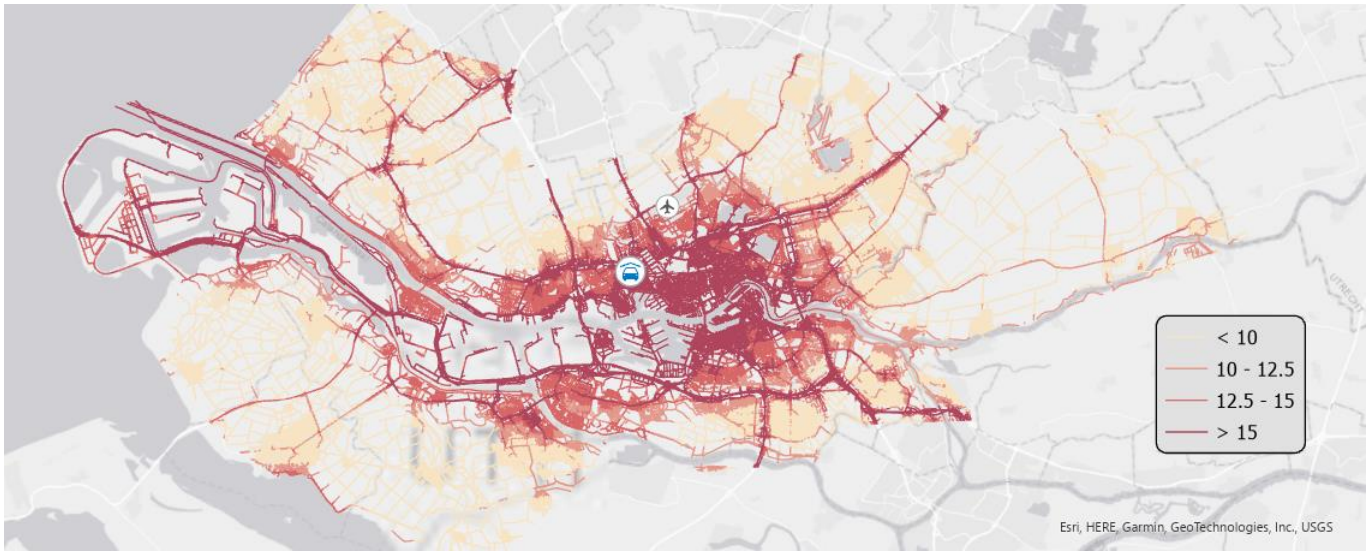

Figure 5.17. *Summer NO_2 LUR model.*

RI-URBANS (www.RIURBANS.eu) is supported by the European Commission under the Horizon 2020 – Research and Innovation Framework Programme, H2020-GD-2020, Grant Agreement number: 101036245

5.6 Variability in 1 km grid cells

The NSD average over the domains is 0.15 for BC (IR: 0.11-0.17), 0.15 for NO_2 (IQR: 0.23-0.18) and 0.18 for UFP (IQR: 0.12-0.18) (see Figure 5.18). The NSD average over the city centre only were higher for UFP: 0.23 (IQR: 0.14-0.25), and NO_2: 0.17 (IQR: 0.12_0.20).

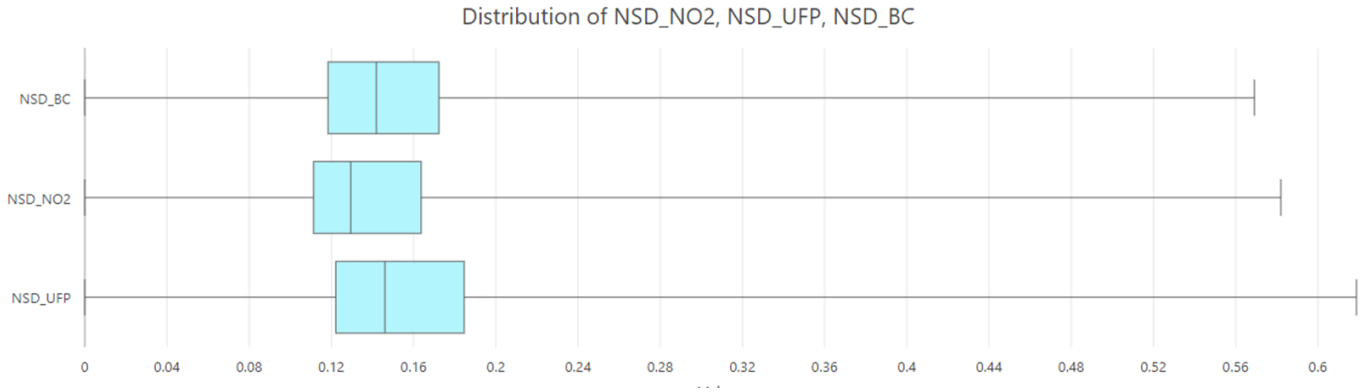

Figure 5.18. *Distribution NSD entire region.*

Within sub-grid variability is the highest for UFP, though only slightly higher as BC and NO_2. This comes mainly from huge concentrations on highways and major arteries in the city. Figure 5.20 clearly shows the cells with highway running through. As UFP coagulates quickly, variation within 1km can be very large. In previous mobile monitoring papers, we also found UFP had the largest within street segment variation.

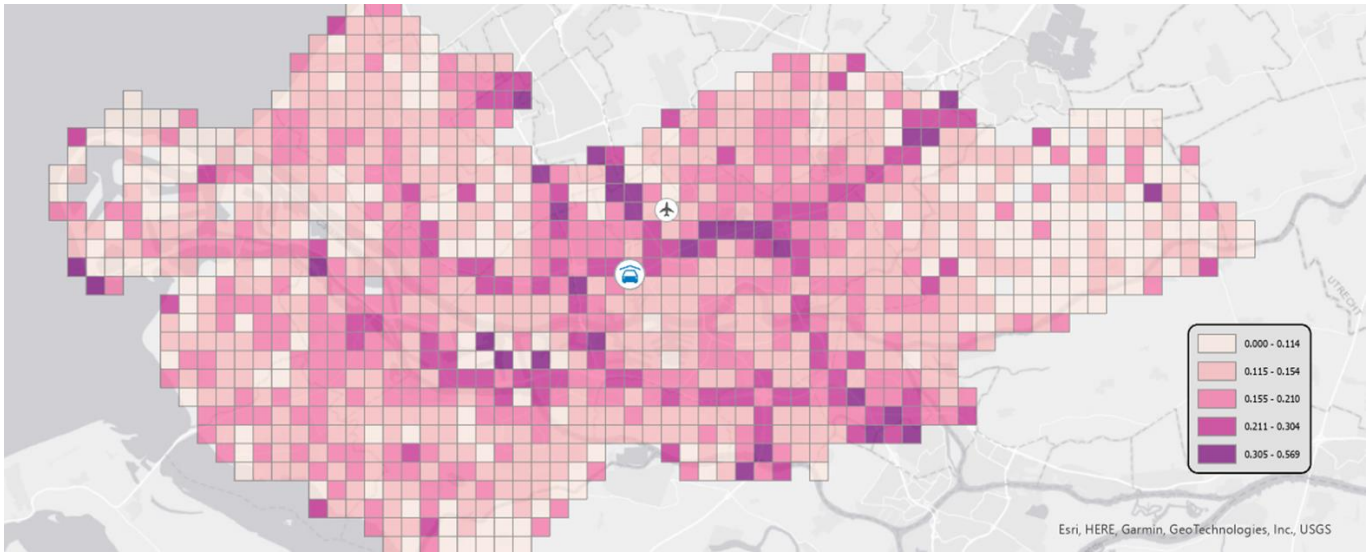

Figure 5.19. *NSD Map for BC.*

RI-URBANS (www.RIURBANS.eu) is supported by the European Commission under the Horizon 2020 – Research and Innovation Framework Programme, H2020-GD-2020, Grant Agreement number: 101036245

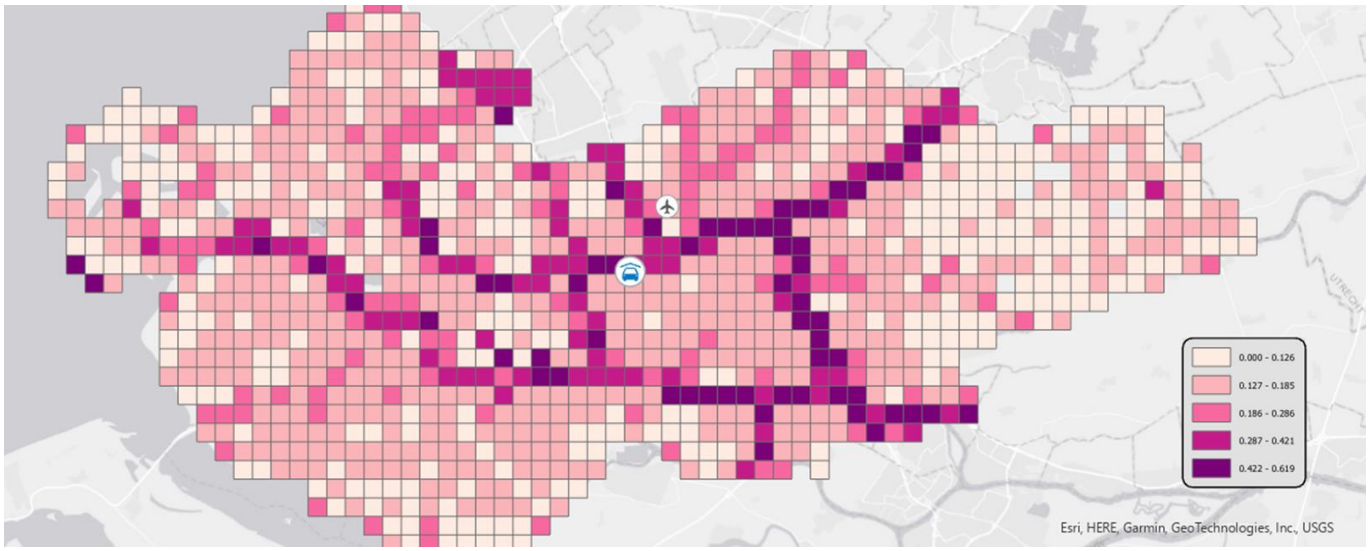

Figure 5.20. *NSD map for UFP.*

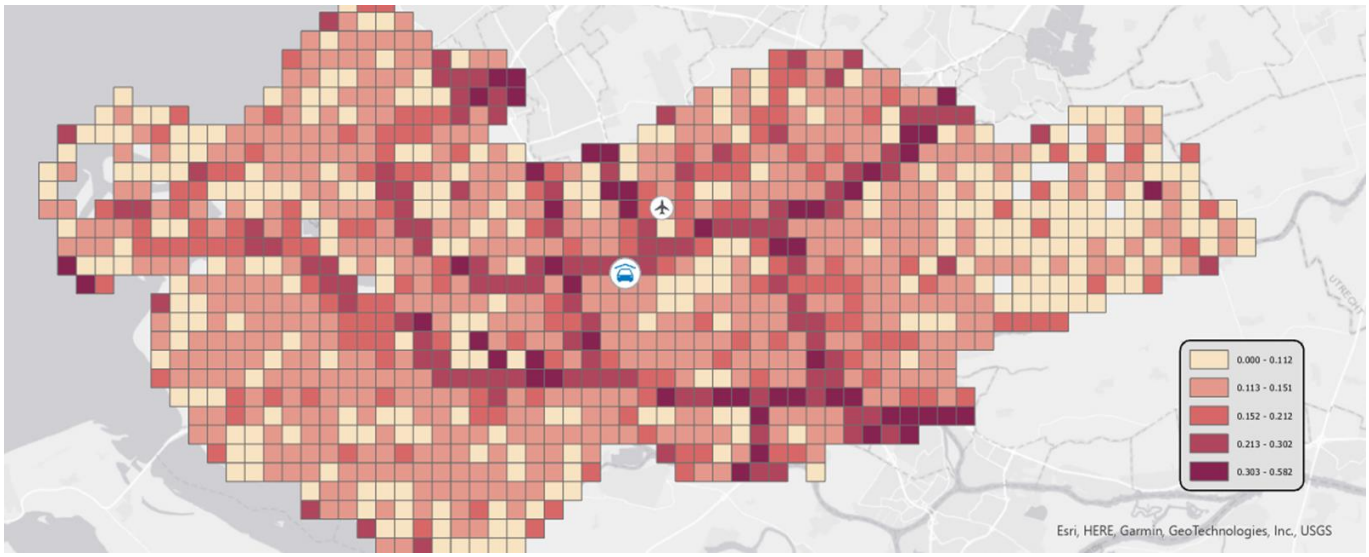

Figure 5.21. *NSD map for NO_2.*

6. Bucharest Pilot

6.1 Mobile measurements and data

Two mobile measurements campaigns representative for Summer and Winter periods have been conducted in Bucharest on 100 km route. The route included heavy traffic roads inside the city, residential, industrial and commercial areas, as well as sub-urban areas. Portable instruments for UFP, different particle matter fractions (PM_1, $PM_{2.5}$, PM_{10}) and gaseous compounds (NO_2) have been used during both campaigns. The car measurements took place in the following timeframes: May – July (Summer period) and January -February (Winter period).

The measurements duration during one route were approximatively 8 hours starting from 8:30 AM local time in order to catch rush hours, but also less intense traffic during the mid-day of working days. At least full 15 measurements routes were performed during each campaign, in different temperature conditions representative for the specific season.

RI-URBANS (www.RIURBANS.eu) is supported by the European Commission under the Horizon 2020 – Research and Innovation Framework Programme, H2020-GD-2020, Grant Agreement number: 101036245

6.2 Model

The ESCAPE Land Use Regression model, together with PyLUR tool and QGIS, was set up in order to retrieve the pollutants maps during both season in Bucharest city. The goal is to retrieve the air pollution maps for Bucharest area in order to assess the contribution of diverse area to air pollution, the gradients on particle concentrations between areas and related exposure along roads in different seasons or atmospheric conditions. The mixed effect model has been also tested, using the mean value from the fixed effect model (LUR) together with the pollutant variability (intercept of mean standard deviation values) for all individual street segments at 1 minute. Individual maps at 100 m grid have been retrieved for each season.

6.3 Maps based on car measurements

6.3.1 Regional variability of different pollutants

Figure 6.1, Figure 6.2, Figure 6.3 and Figure 6.4 represent maps of spatial variability for NO_2, PM_{10}, $PM_{2.5}$ and UFP during Summer and Winter periods in Bucharest. All particulate matter concentrations present higher loadings during the Winter period, with decreased gradients. The PM_{10} sources seem to be well distributed during the Summer period, while the Winter time is characterised by more homogeneous sources. The same behaviour is seen in the case of $PM_{2.5}$ and UFP, where during cold periods only few punctual sources are distinguished. Significant concentrations are highlighted for the particle concentration mainly on the industrial area and anthropogenic agglomerations, but also on some important traffic routes as well. The spatial variation of particles in the city area is significant, with an important number of small particles and high mass concentration of bigger particles in the high populated residential areas (West and South of the city). The average UFP number concentration along the mobile route presents a large spatial gradient mostly during the Summer time, with differences up to a factor of 2 in the mean, which highlights the personal exposure to ultrafine particles along the roads.

The NO_2 concentration presents a higher gradient during warm periods, when the concentrations are higher on the main roads. A less street-confined concentration during the cold periods is observed. On both seasons the main streets, including the Bucharest ring road, represents the main NO_2 source. Also, the city centre roads are highlighted, where the intensity of the traffic persists for the entire day. Seasonal variations of pollutants are also related to the height of the planetary boundary layer, linked to Summer and Winter.

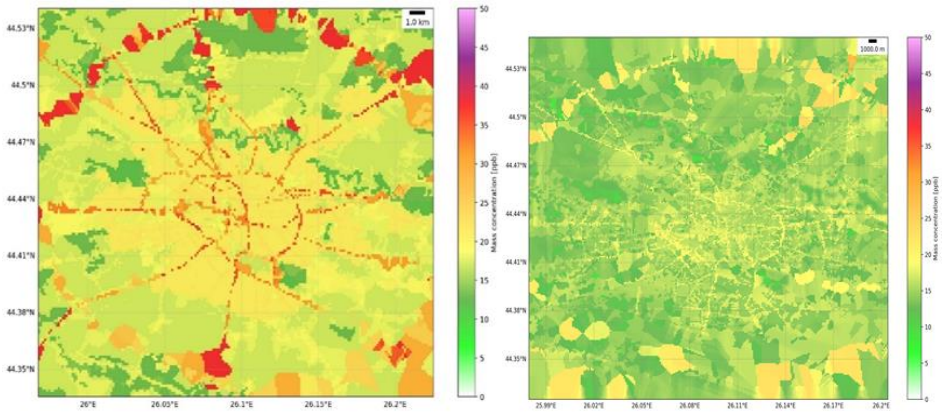

Figure 6.1. *Model maps for NO2 concentration levels in Bucharest during Summer and Winter period.*

RI-URBANS (www.RIURBANS.eu) is supported by the European Commission under the Horizon 2020 – Research and Innovation Framework Programme, H2020-GD-2020, Grant Agreement number: 101036245

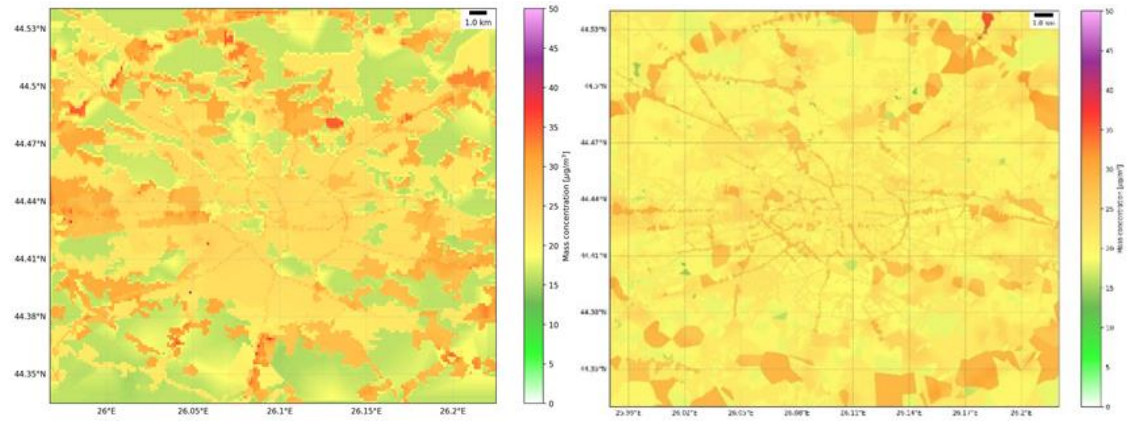

Figure 6.2. *Model maps for PM10 concentration levels in Bucharest during Summer and Winter period.*

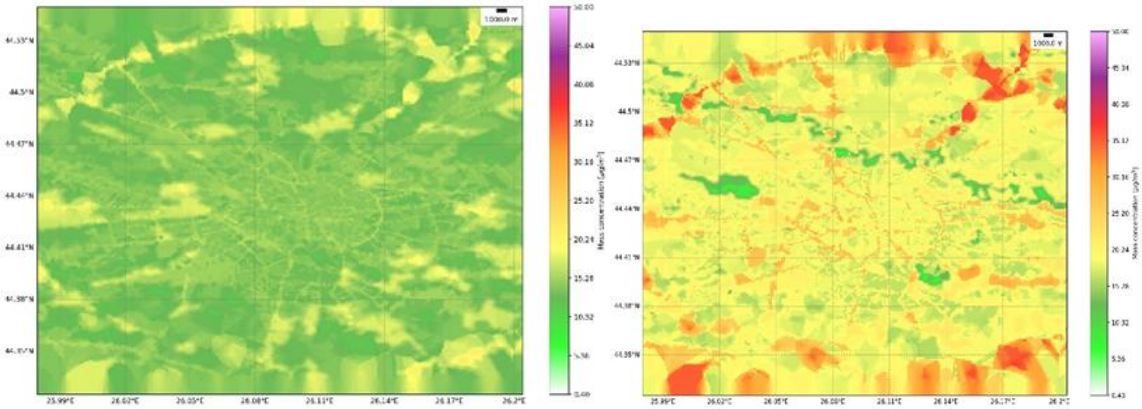

Figure 6.3. *Model maps for $PM_{2.5}$ concentration levels in Bucharest during Summer and Winter period.*

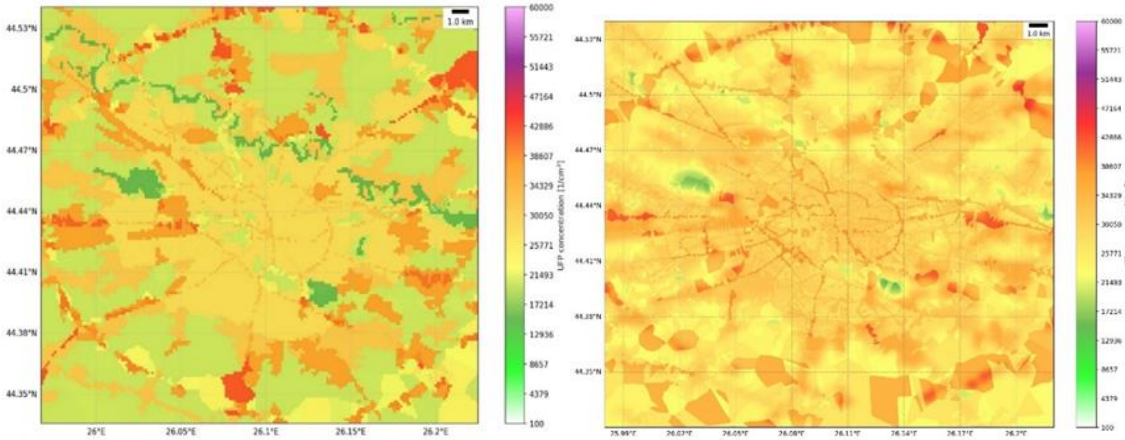

Figure 6.4. *Model maps for UFP concentration levels in Bucharest during Summer and Winter period.*

6.3.2 Evaluation of the Summer and Winter mapping by comparison to fixed measurements

The model performance has been evaluated for NO_2 and PM_{10} concentrations using the hourly data available at the Romanian National Air Quality Monitoring Network (ANPM-8 fix stations representative for urban, industrial and suburban areas) and at MARS supersite, which is part of RADO-Bucharest ACTRIS site (PM_{10}/NO_2 for Winter). The average concentration for each pollutant at fixed stations are represented by circle, the area being proportional

RI-URBANS (www.RIURBANS.eu) is supported by the European Commission under the Horizon 2020 – Research and Innovation Framework Programme, H2020-GD-2020, Grant Agreement number: 101036245

with the concentration (Figure 6.5, Figure 6.6). As expected, the higher average NO_2 concentration at fixed stations are depicted on the traffic areas, while PM_{10} concentrations are higher on urban and sub-urban areas.

Mean values of root mean square error (RMSE), Mean Fractional Bias (MFB) and Mean Fractional Error (MFE) are evaluated using the data from May-August 2022 and January-February 2023 (timeframe of the mobile measurements). Overall, the model performed well, NO_2 values are overestimated, while PM_{10} levels are slightly underestimated (Table 6.1).

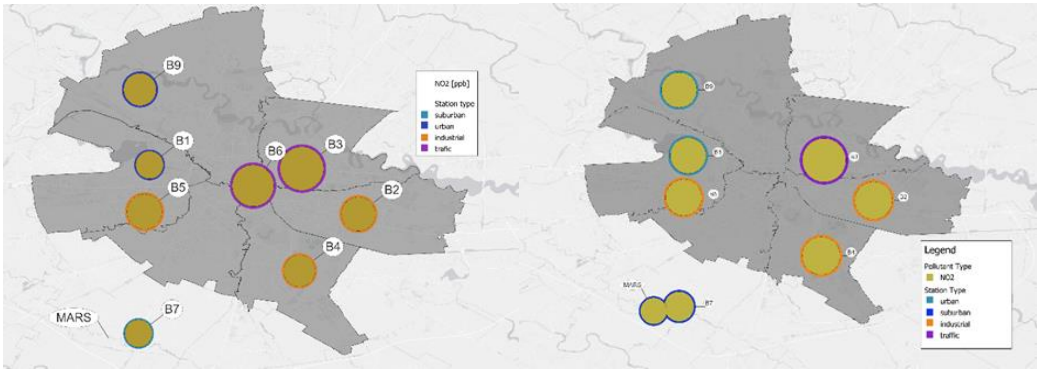

Figure 6.5. *Average concentration of NO_2 during Summer and Winter at fixed sites.*

Figure 6.6. *Average concentration of PM_{10} during Summer and Winter at fixed sites.*

Table 6.1. *Model performance metrics for NO_2 and PM_{10} predicted concentration levels in Bucharest during warm period 2022 and cold period 2023, when compared with measurements from fixed sites.*

Pollutant	Season	Observed mean concentration	Modelled mean concentration
NO_2	***Summer***	12.58 ± 7.71 ppb	20.35 ± 0.70 ppb
	Winter	15.98 ± 9.52 ppb	17.17±0.74 ppb
PM_{10}	***Summer***	24.64±13.18 µg/m^3	22.94 ± 0.45 µg/m^3
	Winter	26.33 ±18.50µg/m^3	27.81± 5.13 µg/m^3

RI-URBANS (www.RIURBANS.eu) is supported by the European Commission under the Horizon 2020 – Research and Innovation Framework Programme, H2020-GD-2020, Grant Agreement number: 101036245

The model overestimated the concentrations for NO_2, while for PM_{10} modelled data agree with the mean values measured at the fixed stations. The mean NO_2 concentration of the modelled data are within the variability of the measurements, given by the standard deviation. The street network in Bucharest is very dense and the distance from the street to residential or industrial areas is very small sometimes (< 5 m), the NO_2 100 x 100 m grid resolution not always capturing all variability. NO_2 concentrations are higher near busy roads due to the large number of vehicles emitting NO. Moreover, NO_2 concentrations are higher on sunny days, due to the conversion of NO to NO_2 in the presence of solar radiation and O_3.

6.3.3 Variability within 1 km x 1km areas

Winter and Summer maps for the normalised standard deviation (NSD) have been computed for all pollutants in order to assess the spatial sub-grid variability of concentrations within 1 km x 1 km areas (Figure 6.7, Figure 6.8, Figure 6.9, Figure 6.10). A higher variability of pollutants concentrations is observed during the Summer period, in the Wintertime important variation are highlighted mostly on the ring road areas.

Similar variability patterns are observed for the particle's concentrations. Higher mean NSD values are observed during Winter in the case of PM_{10} and $PM_{2.5}$, while UFP and NO_2 mean NSD are higher during Summer.

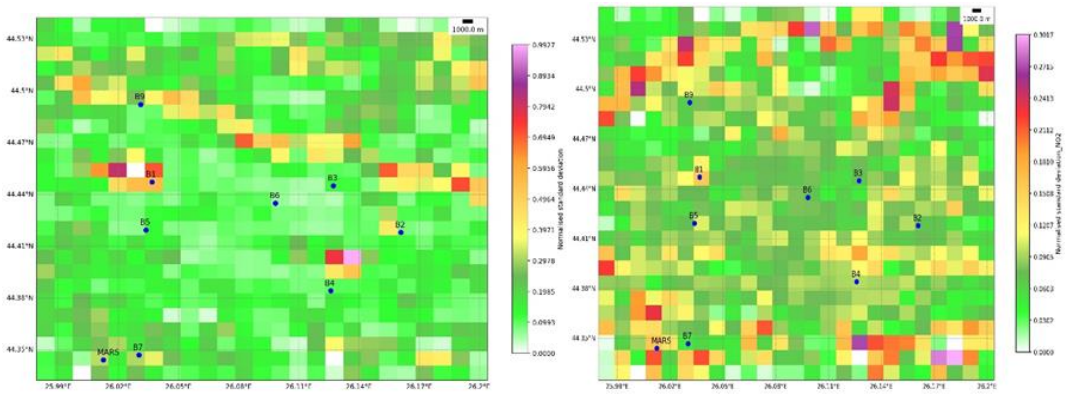

Figure 6.7. *Normalised Standard Deviation of the sub-grids for NO2 concentration levels in Bucharest during Summer and Winter period.*

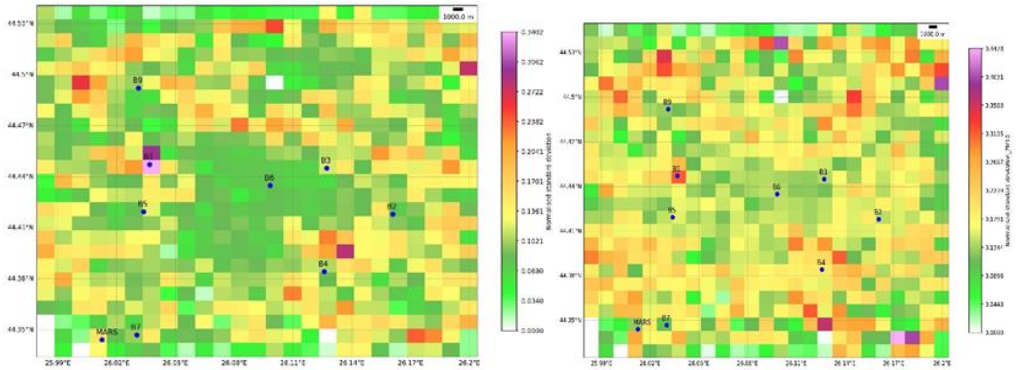

Figure 6.8. *Normalised Standard Deviation of the sub-grids for PM10 concentration levels in Bucharest during Summer and Winter period.*

RI-URBANS (www.RIURBANS.eu) is supported by the European Commission under the Horizon 2020 – Research and Innovation Framework Programme, H2020-GD-2020, Grant Agreement number: 101036245

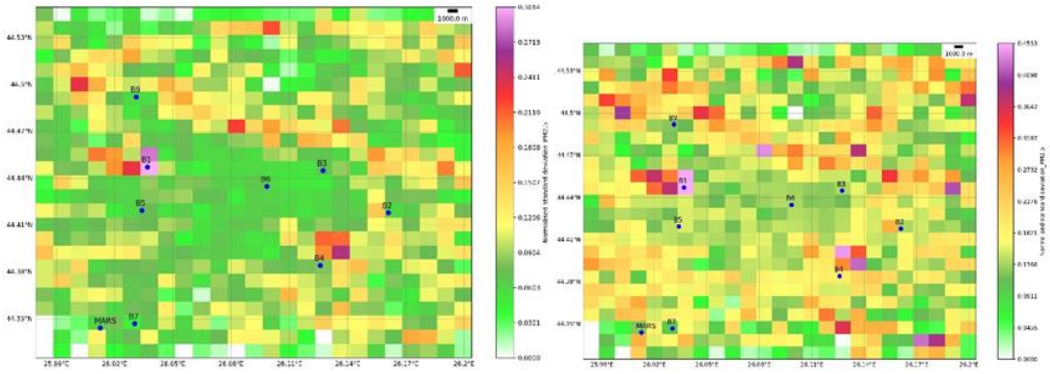

Figure 6.9. *Normalised Standard Deviation of the sub-grids for $PM_{2.5}$ concentration levels in Bucharest during Summer and Winter period.*

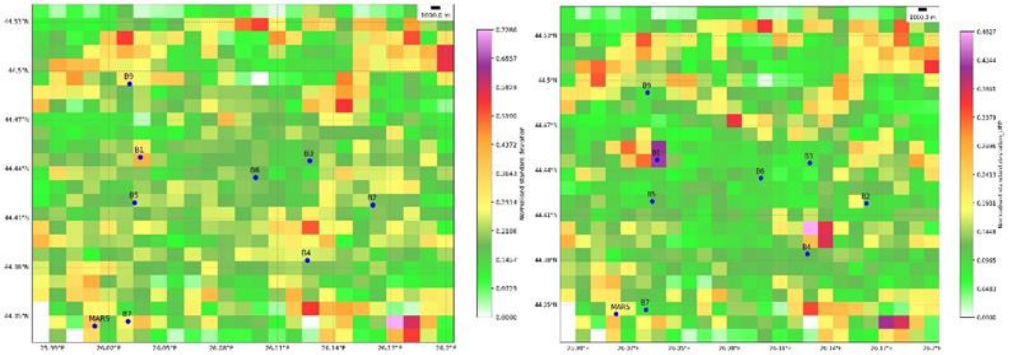

Figure 6.10. *Normalised Standard Deviation of the sub-grids for UFP concentration levels in Bucharest during Summer and Winter period.*

Table 6.2. *Averaged model Normalised Standard Deviation for each pollutant on Summer and Winter periods.*

Pollutant	Mean NSD		Min NSD		Max NSD	
	Summer	Winter	Summer	Winter	Summer	Winter
PM_{10}	0.110	0.165	0.0012	0.0020	0.340	0.448
$PM_{2.5}$	0.088	0.168	0.0010	0.0019	0.301	0.455
UFP	0.209	0.132	0.0001	0.0032	0.729	0.483
NO_2	0.178	0.101	0.0113	0.0032	0.993	0.304

6.3.4 Variability within specific areas

Mean model concentrations on specific areas, as well as concentrations on the same areas from fixed stations are presented in Figure 6.11 and Figure 6.12 for NO_2 and PM_{10}, respectively.

Higher differences of concentrations are depicted between seasons and between model and measurements for NO_2. Lower concentrations of NO_2 was attributed to urban category, while the highest corresponds to traffic as expected. The modelled data presents higher NO_2 concentrations for the Summer period. The Traffic type presents the lower variability during seasons and model/measurements. The relative differences for both model and measurements are less than 40%.

RI-URBANS (www.RIURBANS.eu) is supported by the European Commission under the Horizon 2020 – Research and Innovation Framework Programme, H2020-GD-2020, Grant Agreement number: 101036245

Particulate matter concentration for urban, industrial and traffic types show small differences between seasons and by modelled and measurement data. PM_{10} higher concentrations are observed on modelled data during Winter, with lower concentration for the Industrial type on both modelled and measured data. PM_{10} concentrations present a lower variability with relative differences less than 20%. Normalised Standard Deviation relative differences for these three area types show large differences for UFP.

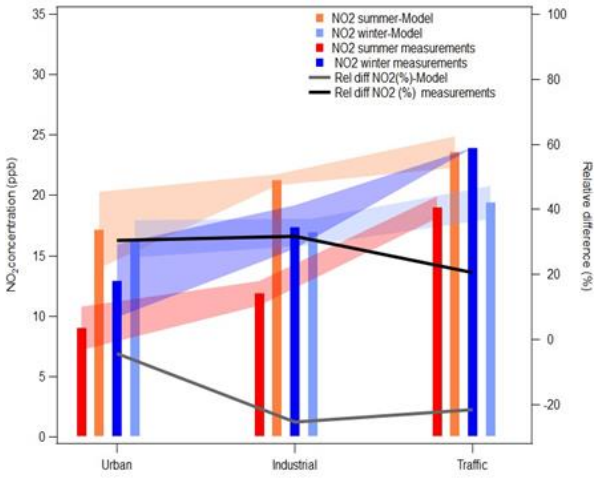

Figure 6.11. *Model versus measurements mean concentrations of NO_2 during Summer and Winter, along with relative difference.*

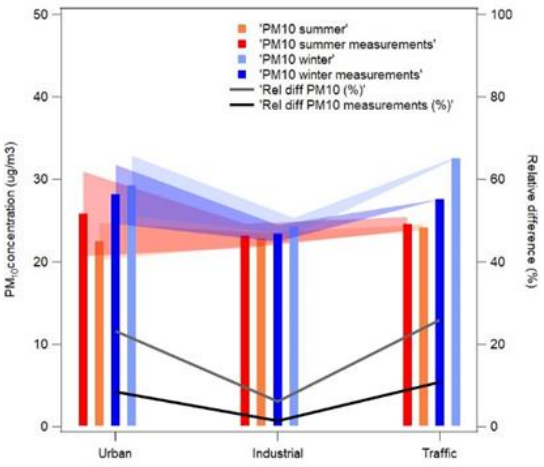

Figure 6.12. *Model versus measurements mean concentrations of PM_{10} during Summer and Winter, along with relative difference.*

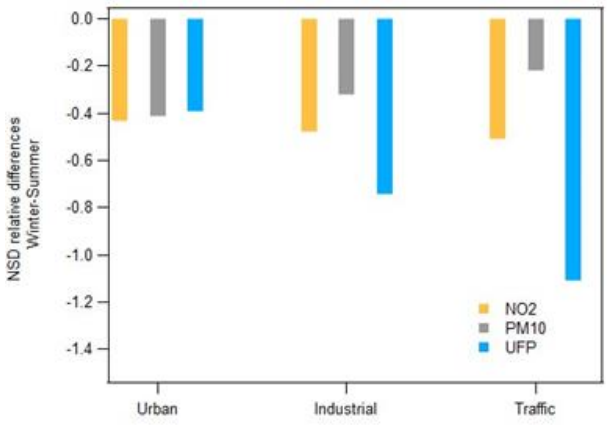

Figure 6.13. *Model NSD relative difference Winter- Summer on different area types.*

6.3.5 Variability between pollutants

Seasonal variation in fine particle fraction ($PM_{2.5}/PM_{10}$) shows higher levels during the Wintertime, which could be related to the increased household heating and small particle generation. The highest fine particle fraction values occur in Winter with ratios around 1, fine particles representing up to 90% from the PM_{10} concentration. During Summer the fine particle fraction is around 0.70, the small particles representing also a high proportion (Figure 6.14).

RI-URBANS (www.RIURBANS.eu) is supported by the European Commission under the Horizon 2020 – Research and Innovation Framework Programme, H2020-GD-2020, Grant Agreement number: 101036245

The main road areas present the highest concentrations of pollutants, both gases and particles concentrations having the highest concentrations on the West side of Bucharest.

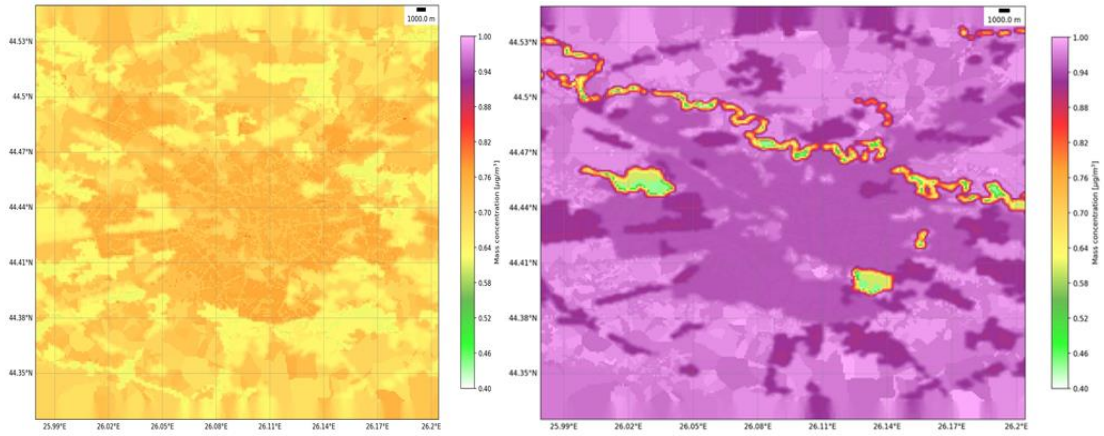

Figure 6.14. *Map of $PM_{2.5}/PM_{10}$ ratio during Summer and Winter.*

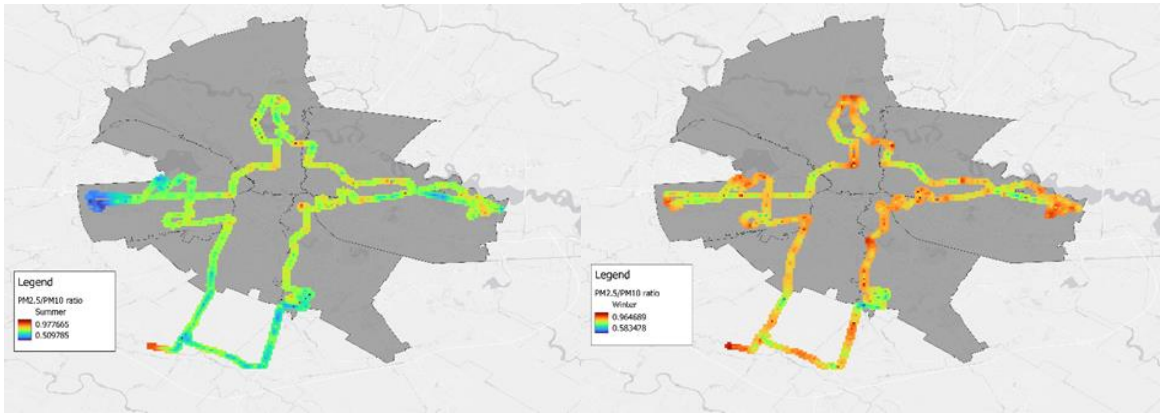

Figure 6.15. *$PM_{2.5}/PM_{10}$ ratio during Summer and Winter along car route.*

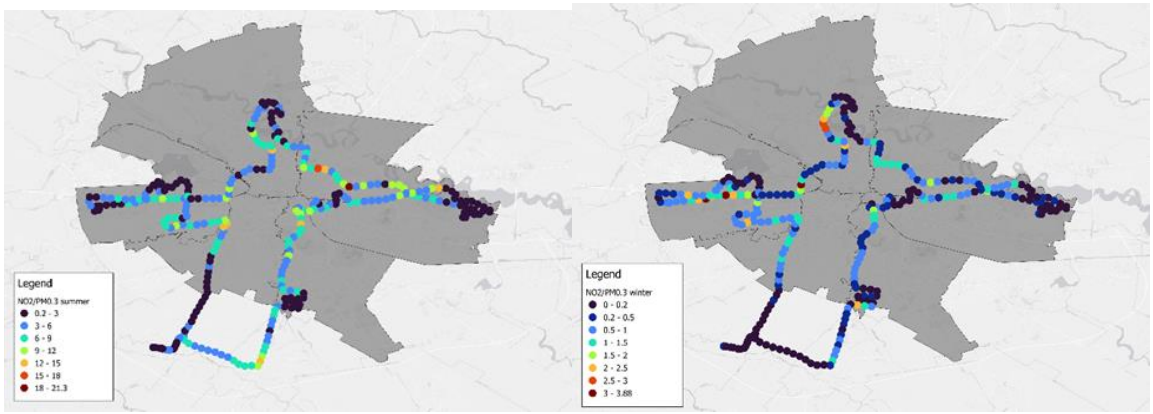

Figure 6.16. *NO_2/UFP ratio during Summer and Winter along car route.*

RI-URBANS (www.RIURBANS.eu) is supported by the European Commission under the Horizon 2020 – Research and Innovation Framework Programme, H2020-GD-2020, Grant Agreement number: 101036245

7. Summary and Outlook

We piloted mapping of air pollution in European cities (Athens, Bucharest, Paris and Rotterdam). The analysis was done for two periods, Winter and Summer and we explored the differences between these two seasons as a comparison.

As a summary of the results from the pilots, for NO_2, the concentrations were higher in Winter than in Summer in Birmingham and in the urban background of Paris and Athens. However, they are similar at traffic sites in Paris and Athens. The higher urban background NO_2 concentrations in Athens and Paris may be linked to lower boundary layer height during Winter than Summer, decreasing the volume in which city emissions are diluted. The influence may not be seen at traffic stations, because NO_X emissions are for a large part emitted by traffic and as NO. The NO emissions are transformed into NO_2 locally by photochemistry. Photochemistry is higher in Summer than in Winter, leading to higher local-NO_2 production in Summer. However, concentrations in streets are also influenced by the urban background. Hence, the higher local-NO_2 production in Summer is counterbalanced by the higher urban background NO_2 in Winter. In Rotterdam and Bucharest, the concentrations of NO_2 tend to be similar in Winter and Summer, probably because the measurements are performed using localized sensors, which may better represent the local-scale than urban background variations.

For particle mass, BC and $PM_{2.5}$, concentrations are higher in Winter than in Summer in all cities probably because of lower boundary layer height, and residential heating emissions. For particle number, concentrations are higher in Winter in Paris, Birmingham and Bucharest, but the concentrations are similar in Winter and Summer in Rotterdam.

In the mapping, we utilized several techniques. The concentrations mapped using the different approaches are compared to measurements performed at fixed stations. Averaged concentrations are compared at urban background sites and traffic sites when possible. For cities using the mixed-LUR approach, such as Bucharest and Rotterdam, the comparison focuses on mean concentrations and their variations. For cities using deterministic modelling, more detailed statistics of comparisons, as daily concentrations were computed.

The model performance goal of Boylan and Russell (2006) was met over Paris for NO_2, $PM_{2.5}$, BC and PN, except for BC in Winter where only the model performance goal is met. For all pollutants in all seasons, the FAC2 is high: 88-93 for NO_2, 63-93 for BC, for 81-97 $PM_{2.5}$ and 95-100 PN. Note that there is no traffic station to evaluate PN concentrations in Winter. For Birmingham, the mean concentrations compare well to the measurements, the MFB are low for NO_2 and $PM_{2.5}$, and the FAC2 is high: 77-82 for NO_2, 76-86 for $PM_{2.5}$, 61-69 for PN. However, there is no traffic station to evaluate PN and only one urban background station for PN. Over Athens, the model performance goal is met in Summer for NO_2 and $PM_{2.5}$, but NO_2 is underestimated in the Winter and in the urban background in the Summer time. There is no urban background measurement of $PM_{2.5}$ in Winter.

Concerning the variability of concentrations, the range of average values for the NSD of NO_2, BC and $PM_{2.5}$ tends to be similar between the different cities, indicating that the variations of the concentrations are of the same order. In Paris, Birmingham and Athens, the NSD is lower for $PM_{2.5}$ than for NO_2, indicating that the variations within the city of NO_2 are higher than those of $PM_{2.5}$. In Paris, the NSD is also high for BC compared to $PM_{2.5}$. This is because NO_2 and BC are largely emitted by traffic, whereas the sources of $PM_{2.5}$ and pathways of formation are more diverse. For NO_2, the average NSD ranges between 0.14 and 0.27 over Paris, 0.14 and 0.36 over Birmingham, 0.16 and 0.19 over Athens, 0.11 and 0.20 over Rotterdam, 0.10 and 0.18 over Bucharest. For $PM_{2.5}$, the average NSD ranges between 0.06 and 0.07 over Paris, between 0.05 and 0.09 over Birmingham, and between 0.09 and 0.17 over Bucharest. It is 0.01 in Athens, but with large variations within the city. Similar NSD ranges for $PM_{2.5}$ and NO_2 in Bucharest may indicate that the traffic sources contribute significantly to $PM_{2.5}$ emissions in Bucharest. For BC, the average NSD is about 0.27 in Paris, and it ranges between 0.11 and 0.17 in Rotterdam. The higher NSD observed in

RI-URBANS (www.RIURBANS.eu) is supported by the European Commission under the Horizon 2020 – Research and Innovation Framework Programme, H2020-GD-2020, Grant Agreement number: 101036245

Paris than in Rotterdam could be related to differences in the traffic fleet. For PN, the NSD ranges between 0.25 and 0.29 in Paris, 0.026 and 0.060 in Birmingham, 0.12-0.25 in Rotterdam, 0.132 and 0.209 in Bucharest. The NSD values are lower by a factor at least 10 in Birmingham than in Paris and Rotterdam, probably because aerosol dynamics (condensation/evaporation and coagulation) was not considered in Birmingham. These processes may be partly responsible for the large PN variability observed. The large NSD in Paris, Rotterdam and Bucharest indicates the large variability of PN and the probably fairly strong influence of traffic sources.

The NSD detailed above are averaged over cities, but they can reach higher values, especially in districts where there are large roads. The large values simulated for NO_2, BC and PN show that the concentrations of these pollutants vary largely within cities. Variations of $PM_{2.5}$ are lower.

To analyse further the variability of pollutants, the ratio of NO_2, BC and BC, PN were computed in Paris and Rotterdam based on quantile division. In Paris, low NO_2, BC and PN were observed in areas far from the roads. In Rotterdam, high NO_2 concentrations were more restricted to the city centre, UFP was most pronounced on the major roads and BC was relatively elevated in the suburbs. In Birmingham, higher ratios between predicted NO_2 and $PM_{2.5}$ or PN were more restricted to the city centre and areas near motorways, which were more influenced by higher traffic induced NO_2. In Athens, $NO_2/PM_{2.5}$ were predicted high mainly over the road network.

The Normalised Mean Bias (NMB), which quantifies the differences between the sub-grid variability and the regional-scale urban background concentrations simulated with a chemistry-transport model (CTM) of 1 km x 1 km resolution, is higher over Paris for NO_2, BC, PN (between 36% and 87%) than $PM_{2.5}$ (about 9%), in agreement with the higher NSD. It is the highest for BC (between 75% and 87%).

To estimate the population exposure to air pollution over Paris, the MAJIC database was used to estimate the number of inhabitants in each building. People living in a building that is on the main street are assigned to that street concentration. People living in a building that does not open directly onto the street are assigned to urban background concentrations. The Exposure Scaling Factor (ESF) is defined as the ratio of the PWC to the regional scale concentration. The ESF is the highest for NO_2, BC, PN, and $PM_{2.5}$ in order, and the average ESF in Paris is higher than 1 for all pollutants in both Summer and Winter. The ESF is the highest for BC (about 1.3), indicating that outdoor population exposure is under-estimated by as much as 30% when considering urban background concentrations with a resolution of 1 km x 1 km. The ESF is the closest to 1 for $PM_{2.5}$ (1.03 to 1.04). Over Athens, the exposure is determined using 100 m^2 spatial resolution for the population and for the model subgrid representation. The domain-averaged ESF value is equal to 1 for $PM_{2.5}$, as the variability of $PM_{2.5}$ is low within the city. However, an ESF value lower than 1 is obtained for NO_2. The main difference between Paris and Athens lies in the representation of the subgrid variability. As a gaussian-based approach is superimposed to the road network, the subgrid concentrations (100 m^2) can be lower than the main grid (1000 m^2) concentrations. In the eulerian street-network approach used in Paris, subgrid local-scale concentrations are not averaged over 100 m^2 grid cells, but local-scale concentrations are averaged within each street segment, leading to local-scale street concentrations always higher than background concentrations and ESF values much higher than 1 for NO_2, BC and PN.

As the outlook from this deliverable, the methods of spatial air quality mapping is suggested as one of the service tools of RI-URBANS and elaborated in the follow-up documentation within the project.

RI-URBANS (www.RIURBANS.eu) is supported by the European Commission under the Horizon 2020 – Research and Innovation Framework Programme, H2020-GD-2020, Grant Agreement number: 101036245

7. References

Hanna, S. and Chang, J.: Acceptance criteria for urban dispersion model evaluation, Meteorol. Atmos. Phys., 116, 133–146, 2012.

Karl, M., Walker, S.-E., Solberg, S., and Ramacher, M. O. P.: The Eulerian urban dispersion model EPISODE – Part 2: Extensions to the source dispersion and photochemistry for EPISODE–CityChem v1.2 and its application to the city of Hamburg, Geosci. Model Dev., 12, 3357–3399, https://doi.org/10.5194/gmd-12-3357-2019, 2019.

Kerckhoffs, J., Khan, J., Hoek, G., Yuan, Z., Ellermann, T., Hertel, O., Ketzel, M., Jensen, S. S., Meliefste, K., & Vermeulen, R. (2022). Mixed-Effects Modeling Framework for Amsterdam and Copenhagen for Outdoor NO2 Concentrations Using Measurements Sampled with Google Street View Cars. *Environmental Science & Technology*, *56*(11), 7174-7184. https://doi.org/10.1021/acs.est.1c05806

Kim, Y., Lugon, L., Maison, A., Sarica, T., Roustan, Y., Valari, M., Zhang, Y., André, M., and Sartelet, K.: MUNICH v2.0: a street-network model coupled with SSH-aerosol (v1.2) for multi-pollutant modelling, Geosci. Model Dev., 15, 7371–7396, https://doi.org/10.5194/gmd-15-7371-2022, 2022.

Létinois, 2014. Méthodologie de répartition spatiale de la population. Rapport LCSQA, http://www.lcsqa.org/rapport/2014/ineris/methodologie-repartition-spatiale-population

Lugon L, Sartelet K, Kim Y, Vigneron J, Chrétien O: Simulations of primary and secondary particles in the streets of Paris using MUNICH. Faraday Discussions, http://dx.doi.org/10.1039/D0FD00092B, 2021.

Menut, L., Bessagnet, B., Briant, R., Cholakian, A., Couvidat, F., Mailler, S., Pennel, R., Siour, G., Tuccella, P., Turquety, S., and Valari, M. (2021). The chimere v2020r1 online chemistry-transport model. Geosci. Model Dev., 14(11):6781–6811, https://doi.org/10.5194/gmd-14-6781-2021

Sartelet K., Couvidat F., Wang Z., Flageul C., Kim Y. (2020), SSH-Aerosol v1.1: A Modular Box Model to Simulate the Evolution of Primary and Secondary Aerosols. Atmosphere, 2020, 11, 525, https://doi.org/10.3390/atmos11050525.

Sartelet, K., Kim, Y., Couvidat, F., Merkel, M., Petäjä T., Sciare J. and Wiedensohler, A. (2022), Influence of emission size distribution and nucleation on number concentrations over Greater Paris. Atmos. Chem. Phys., 22, 8579-8596, https://doi.org/10.5194/acp-22-8579-2022.

Savadhooki Savadkoohi, M., Pandolfi, M., Reche, C., Niemi, J., Mooibroek, D., Titos, G., Green, D., Tremper, A., Hueglin, C., Liakakou, E., Mihalopoulos, N., Stavroulas, I., Artiñano, B., Coz, E., Alados-Arboledas, L., Beddows, D., Riffault, V., Brito, J., Bastian, S., Baudic, A., Colombi, C., Costabile, F., Chazeau, B., Marchand, N., Gómez-Amo, J., Estellés, V., Matos, V., Gaag, E., Gille, G., Luoma, K., Manninen, H., Norman, M., Silvergren, S., Petit, J., Putaud, J., Rattigan, O., Timonen, H., Tuch, T., Merkel, M., Weinhold, K., Vratolis, S., Vasilescu, J., Favez, O., Harrison, R., Laj, P., Wiedensohler, A., Hopke, P., Petäjä, T., Alastuey, A., and Querol, X. The variability of mass concentrations and source apportionment analysis of equivalent black carbon across urban europe. Environ. Int., 178:108081, 2023

Zhong, J, Hood, C, Johnson, K, Stocker, J, Handley, H, Wolstencroft, M, Mazzeo, A, Cai, X & Bloss, W J (2021). Using task farming to optimize a street-scale resolution air quality model of the West Midlands (UK). Atmosphere, 12(8), 983.

Zhong, J., Harrison, R. H., Bloss, W. J., Visschedijk, A. and Gon H. D. V. (2023). Modelling the dispersion of particle number concentrations in the West Midlands, UK using the ADMS-Urban model, Environment International, 181,108273.

RI-URBANS (www.RIURBANS.eu) is supported by the European Commission under the Horizon 2020 – Research and Innovation Framework Programme, H2020-GD-2020, Grant Agreement number: 101036245